cmgh
CELLULAR AND MOLECULAR GASTROENTEROLOGY AND HEPATOLOGY

ORIGINAL RESEARCH

p53-Independent Induction of p21 Fails to Control Regeneration and Hepatocarcinogenesis in a Murine Liver Injury Model

Laura Elisa Buitrago-Molina,[1,§] Silke Marhenke,[1,§] Diana Becker,[2] Robert Geffers,[3] Timo Itzel,[4] Andreas Teufel,[4] Hartmut Jaeschke,[5] André Lechel,[6] Kristian Unger,[7] Jovana Markovic,[1] Amar Deep Sharma,[1] Jens U. Marquardt,[2] Michael Saborowski,[1] Anna Saborowski,[1,§] and Arndt Vogel[1,§]

[1]Department of Gastroenterology, Hepatology and Endocrinology, Hannover Medical School, Hannover, Germany; [2]First Department of Medicine, University Hospital Schleswig-Holstein, Campus Lübeck, Lübeck, Germany; [3]Department of Cell Biology, Helmholtz Centre for Infection Research, Braunschweig, Germany; [4]Division of Hepatology, Department of Medicine II, Medical Faculty Mannheim, Heidelberg University, Mannheim, Germany; [5]Department of Pharmacology, Toxicology and Therapeutics, University of Kansas Medical Center, Kansas City, Kansas; [6]Department of Internal Medicine I, University Hospital Ulm, Ulm, Germany; [7]Helmholtz Zentrum München, German Research Center for Environmental Health GmbH, Neuherberg, Germany

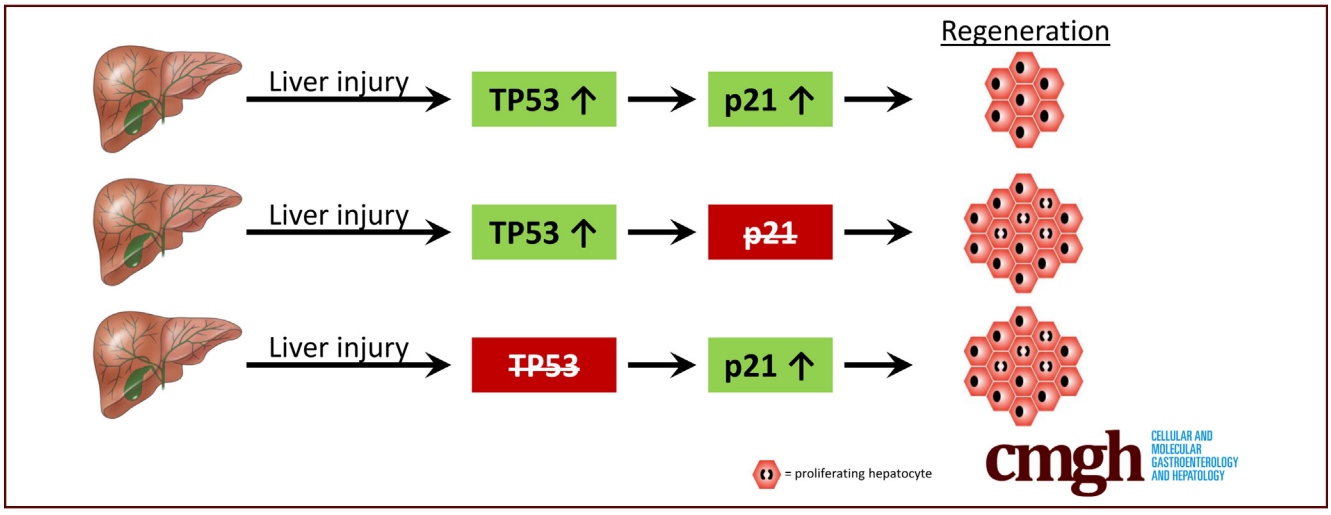

SUMMARY

Functional annotation of individual components of the DNA damage response pathway in the liver shows distinct genotype–phenotype correlations and unveils their complex interplay in response to liver injury.

BACKGROUND & AIMS: A coordinated stress and regenerative response is important after hepatocyte damage. Here, we investigate the phenotypes that result from genetic abrogation of individual components of the checkpoint kinase 2/transformation-related protein 53 (p53)/cyclin-dependent kinase inhibitor 1A (p21) pathway in a murine model of metabolic liver injury.

METHODS: Nitisinone was reduced or withdrawn in *Fah*$^{-/-}$ mice lacking *Chk2*, *p53*, or *p21*, and survival, tumor development, liver injury, and regeneration were analyzed. Partial hepatectomies were performed and mice were challenged with the Fas antibody Jo2.

RESULTS: In a model of metabolic liver injury, loss of *p53*, but not *Chk2*, impairs the oxidative stress response and aggravates liver damage, indicative of a direct p53-dependent protective effect on hepatocytes. Cell-cycle control during chronic liver injury critically depends on the presence of both p53 and its downstream effector p21. In *p53*-deficient hepatocytes, unchecked proliferation occurs despite a strong induction of p21, showing a complex interdependency between p21 and p53. The increased regenerative potential in the absence of p53 cannot fully compensate the surplus injury and is not sufficient to promote survival. Despite the distinct phenotypes associated with the loss of individual components of the DNA damage response, gene expression patterns are dominated by the severity of liver injury, but reflect distinct effects of p53 on proliferation and the anti-oxidative stress response.

CONCLUSIONS: Characteristic phenotypes result from the genetic abrogation of individual components of the DNA damage-response cascade in a liver injury model. The extent to which loss of gene function can be compensated, or affects injury and proliferation, is related to the level at which the cascade is interrupted. Accession numbers of repository for expression

microarray data: GSE156983, GSE156263, GSE156852, and GSE156252. *(Cell Mol Gastroenterol Hepatol 2021;11:1387–1404; https://doi.org/10.1016/j.jcmgh.2021.01.006)*

Keywords: DNA Damage; Oxidative Stress Response; CHK2; HCC.

Exposure to extrinsic factors that directly or indirectly induce DNA damage activates a cascade of response mechanisms in the injured liver. Induction of survival pathways that loosen the breaks on proliferative control in hibernating hepatocytes is critical to enable efficient regeneration and facilitate survival.[1–4] At the same time, maintaining coordinated guidance through the cell cycle is necessary to ensure that survival does not happen at the expense of malignant transformation, which is especially challenging in the face of chronic liver injury. Activation of transformation-related protein 53 (p53) serves as the central mediator of cell-cycle control and as a major barrier against malignant transformation.[5]

Inactivation of DNA damage response checkpoints can influence tumor development. For instance, patients with mutations in ataxia telangiectasia mutated (ATM) are prone to carcinogenesis. Paradoxically, loss of ATM delays carcinogen-induced hepatocarcinogenesis in mice, which has been attributed to a strong compensatory activation of ataxia telangiectasia and Rad3 related, checkpoint kinase (CHK)1, and p53.[6] After double-strand breaks, ATM phosphorylates and activates CHK2, a serine/threonine protein kinase with a variety of substrates, including p53 and cyclin-dependent kinase inhibitor 1A (p21).[7] *CHK2* mutations have been identified in human cancers and loss of CHK2 predisposes transgenic mice to tumorigenesis, although they are not prone to spontaneous cancer development.[8] The role of CHK2 in chronic liver injury and hepatocarcinogenesis is currently unknown.

After activation, p53 orchestrates various biological processes such as cell-cycle arrest, apoptosis, and DNA repair. Extensive damage may trigger apoptosis to eradicate the affected cells or lead to senescence via p21 and cyclin-dependent kinase inhibitor 2A (p16). After milder damage, p53 can transcriptionally activate cell-cycle regulators and facilitate DNA repair and survival. In the murine liver, loss of p53 alone leads to formation of hepatocellular carcinomas with a long latency of 14–20 months, but dramatically accelerates carcinogen- and oncogene-induced tumor development.[2,9,10] Although the capacity of p53 to suppress liver tumor development is well established, increasing evidence supports the context-dependent role of p53 in acute liver diseases. On the one hand, there is evidence—albeit controversial—that p53 protects hepatocytes from acetaminophen-induced liver injury by regulating drug-metabolizing enzymes and initiating liver regeneration.[11,12] On the other hand, activation of p53 has been implicated in the progression of alcoholic and nonalcoholic liver injury by increasing oxidative stress and apoptosis.[13,14]

p21 is one of the main effectors of p53, with considerable tumor–suppressive potential that mediates cell-cycle arrest and senescence in response to DNA damage.[15] However, data from preclinical model systems challenged the view of p21 as an exclusive tumor suppressor.[16] In this regard, we previously showed that the degree of liver injury and the strength of p21 activation determine its effects on hepatocyte proliferation and hepatocarcinogenesis.[17] Deletion of p21 led to continuous hepatocyte proliferation in mice with severe injury, allowing animals to survive, but also resulted in rapid tumor development. In contrast, liver proliferation was reduced and hepatocarcinogenesis was delayed in p21-deficient mice with moderate injury.

The aim of this study was to delineate the role of p53 in relation to its downstream target p21 and its upstream regulator CHK2 during chronic liver disease. We used a metabolic mouse model of hereditary tyrosinemia type 1, which is an autosomal-recessive human disease caused by the genetic inactivation of the fumarylacetoacetate hydrolase (FAH). FAH is expressed mainly in the liver and in the kidneys, where it catalyzes the last step in the tyrosine catabolism pathway. Accumulation of toxic metabolites, such as fumarylacetoacetate (FAA), causes liver injury and severely increases susceptibility to liver cancer development. The drug nitisinone (also known as NTBC) blocks the pathway upstream of the formation of FAA and is used to treat patients with hereditary tyrosinemia type 1. The murine model of *Fah* deficiency recapitulates the phenotypic manifestations of human liver disease.[18–20]

Results

Loss of p53 Does Not Rescue Survival Despite Unchecked Proliferation in Mice With Severe Liver Injury

To study the role of p53 and CHK2 in acute and chronic liver injury, we crossed $Fah^{-/-}$ mice with the $Chk2^{-/-}$ strain (denoted $Fah/Chk2^{-/-}$) or with animals with liver-specific loss of p53 (*AlfpCre;* $p53^{fl/fl}$, denoted as $Fah/p53^{-/-}$). Both double-knockout strains, as well as $Fah^{-/-}$ controls, did not show any overt morphologic or biochemical phenotype within the observational time frame of 15 months when supplemented with 100% NTBC. We previously showed that after NTBC withdrawal, $Fah^{-/-}$ mice die of acute liver failure within 2–4 months, whereas $Fah/p21^{-/-}$ mice survive

§Authors share co-senior authorship.

Abbreviations used in this paper: **aCGH, array comparative genomic hybridization; ATM, ataxia telangiectasia mutated; BCL2, B-cell lymphoma 2; CDK, cyclin-dependent kinase; CHK, checkpoint kinase; FAA, fumarylacetoacetate; FAH, fumarylacetoacetate hydrolase; GSEA, gene set enrichment analysis; GSH, glutathione; GSSG, glutathione disulfide; IP, immunoprecipitation; NRF2, nuclear factor erythroid 2-related factor 2; NTBC, nitisinone; p16, cyclin-dependent kinase inhibitor 2A; p21, cyclin-dependent kinase inhibitor 1A; p53, transformation-related protein 53; RB, retinoblastoma; TUNEL, terminal deoxynucleotidyl transferase–mediated deoxyuridine triphosphate nick-end labeling.**

Most current article

2352-345X
https://doi.org/10.1016/j.jcmgh.2021.01.006

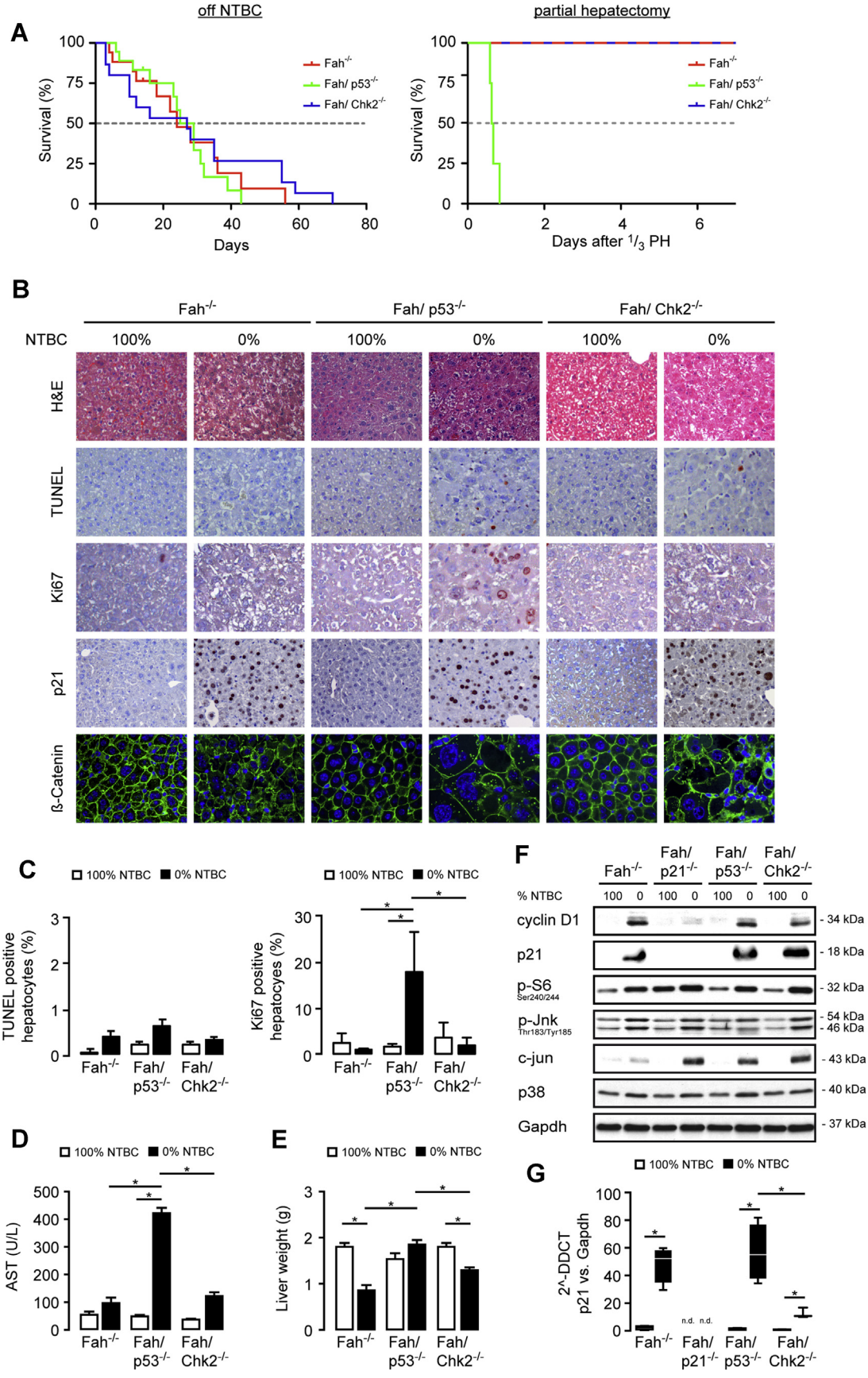
A
off NTBC
partial hepatectomy
Survival (%)
Days
Days after 1/3 PH
Fah-/-
Fah/ p53-/-
Fah/ Chk2-/-
B
NTBC
100%
0%
H&E
TUNEL
Ki67
p21
ß-Catenin
C
100% NTBC
0% NTBC
TUNEL positive hepatocytes (%)
Ki67 positive hepatocyes (%)
D
AST (U/L)
E
Liver weight (g)
F
% NTBC
cyclin D1
p21
p-S6 Ser240/244
p-Jnk Thr183/Tyr185
c-jun
p38
Gapdh
- 34 kDa
- 18 kDa
- 32 kDa
- 54 kDa
- 46 kDa
- 43 kDa
- 40 kDa
- 37 kDa
G
2^-DDCT p21 vs. Gapdh
n.d.

for more than 6 months.[3,17] To assess the consequences of loss of p53 or CHK2 on acute liver injury in *Fah*$^{-/-}$ mice, we withdrew NTBC from 8-week-old *Fah*$^{-/-}$, *Fah/p53*$^{-/-}$, and *Fah/Chk2*$^{-/-}$ mice. All mice eventually died of liver failure, with a median overall survival independent of the presence of p53 or CHK2 (*Fah*$^{-/-}$: median overall survival, 24 d; n = 17; *Fah/p53*$^{-/-}$: median overall survival, 27 d; n = 17; *Fah/Chk2*$^{-/-}$ mice: median overall survival, 26.5 d; n = 26) (Figure 1*A*, left). Characteristic of hepatic injury, liver histology on day 14 after NTBC withdrawal showed multiple small foci of necroinflammation and dysplastic hepatocytes (H&E and β-catenin staining) (Figure 1*B*), and a few scattered terminal deoxynucleotidyl transferase–mediated deoxyuridine triphosphate nick-end labeling (TUNEL)-positive hepatocytes in *Fah*$^{-/-}$ as well as in double-knockout mice (Figure 1*B* and *C*). Although loss of p53 did not affect overall survival, increased transaminase levels indicated that liver injury was most pronounced in the absence of p53 compared with *Fah*$^{-/-}$ and *Fah/Chk2*$^{-/-}$ mice (Figure 1*D*). The injury phenotype of p53-deficient mice was unveiled further when we performed one-third partial hepatectomies in mice taken off NTBC. Although *Fah*$^{-/-}$ and *Fah/Chk2*$^{-/-}$ mice tolerated this additional damaging insult, none of the p53-deficient animals survived beyond day 1 (Figure 1*A*, right).

We previously showed that the near-complete block in proliferation in the hepatocyte compartment of *Fah*$^{-/-}$ mice off NTBC, which is fully reversible after restarting NTBC treatment,[21] is caused by a strong induction of p21.[17] Consequently, genetic loss of p21 resulted in continuous hepatocyte proliferation and a significantly prolonged survival of *Fah/p21*$^{-/-}$ mice taken off NTBC.[3] Although p53 is one of the master regulators of p21, NTBC withdrawal led to a significant up-regulation of p21 messenger RNA and protein expression in both *Fah/p53*$^{-/-}$ and *Fah/Chk2*$^{-/-}$ mice, indicating that p21 was induced independently of p53 and CHK2 (Figure 1*B*, *F*, and *G*). Surprisingly, although only few Ki67-positive cells were detectable in *Fah/Chk2*$^{-/-}$ mice on 0% NTBC similar to *Fah*$^{-/-}$ mice, a large fraction of proliferating hepatocytes was present in *Fah/p53*$^{-/-}$ mice despite the strong induction of p21 (Figure 1*B* and *C*).

To delineate whether proliferation-related pathways show a distinct activation profile in the proliferative vs the non-proliferative genotypes, we generated liver lysates from mice on NTBC and 14 days off NTBC from all groups, including *Fah/p21*$^{-/-}$ mice, and performed immunoblotting for cyclin D1, c-Jun N-terminal kinase/Jun signaling, mechanistic target of rapamycin kinase mediators (ribosomal protein S6 phosphorylation), and p38 (Figure 1*F*). Overall, although this basic characterization coherently showed activated signaling in the 0% NTBC livers compared with the respective 100% NTBC controls, we did not observe any consistent differences between the distinct genotypes that could differentiate between the groups with and without hepatocyte proliferation.

In agreement with the increased liver proliferation phenotype, *Fah/p53*$^{-/-}$ mice were able to maintain their liver weight independent of NTBC withdrawal, whereas the lack of a proliferative response in *Fah*$^{-/-}$ and *Fah/Chk2*$^{-/-}$ mice was accompanied by a significantly reduced liver weight 2 months after NTBC withdrawal (Figure 1*E*).

Taken together, we previously showed that severe liver injury induced by NTBC withdrawal leads to activation of p21, and genetic loss of *p21* enables a strong proliferative response and prolongs survival.[3,17] Here, we show that in the absence of p53, FAA-induced liver injury is aggravated, and is accompanied by increased hepatocyte proliferation, similar to our observation in *Fah/p21*$^{-/-}$ mice. The pronounced expression of p21 in the *Fah/p53*$^{-/-}$ mice indicates that p21 requires intact p53 to induce the profound cell-cycle arrest characteristic of *Fah*$^{-/-}$ mice with liver injury. Despite the strong proliferative response and in contrast to the *Fah/p21*$^{-/-}$ phenotype, *Fah/p53*$^{-/-}$ mice show the same high mortality as *Fah*$^{-/-}$ mice off NTBC. Partial hepatectomy as an additional insult to the liver distinguished the *p53*-deficient from the *Chk2*-deficient and *Fah*$^{-/-}$ control mice. This suggests that the overall potential of the *p53*-deficient liver to compensate for acute liver injury is reduced, but that if the injury does not exceed a certain threshold, compensatory proliferation can partially rescue and protect *Fah/p53*$^{-/-}$ mice from a further increase in early lethality. Unlike loss of *p53*, *Chk2* deficiency neither aggravates FAA-induced liver injury nor alters the proliferative arrest observed in *Fah*$^{-/-}$ mice.

Apoptosis Resistance of Fah$^{-/-}$ *Hepatocytes Is Not Fully Reversed by Loss of Either* p53, Chk2, *or* p21

Fah$^{-/-}$ mice develop a profound resistance against FAS-induced apoptosis after NTBC withdrawal,[22,23] which might

Figure 1. (***See previous page***). **p53 does not affect survival but is required for p21-mediated cell-cycle arrest in *Fah*-deficient mice with severe liver injury.** (*A*) Kaplan–Meier survival curves of *Fah*$^{-/-}$ (n = 17), *Fah/p53*$^{-/-}$ (n = 17), and *Fah/Chk2*$^{-/-}$ (n = 26) mice on 0% NTBC (*left*) and *Fah*$^{-/-}$ (n = 8), *Fah/p53*$^{-/-}$ (n = 4), and *Fah/Chk2*$^{-/-}$ (n = 8) mice after one-third partial hepatectomy (14 days off NTBC, *right*). (*B–F*) Eight-week-old *Fah*$^{-/-}$, *Fah/p21*$^{-/-}$, *Fah/p53*$^{-/-}$, and *Fah/Chk2*$^{-/-}$ mice on 100% NTBC or 14 days after NTBC withdrawal. (*B*) Representative H&E, TUNEL, Ki67, and p21 immunohistochemistry, as well as immunofluorescence staining for ß-catenin. *Fah/p53*$^{-/-}$ livers show numerous Ki67-positive hepatocytes despite strong activation of p21. (*C*) *Left*: The relative percentage of TUNEL-positive hepatocytes was not significantly different between the individual genotypes. Means ± SEM across multiple mice (n = 4–6). *Right*: The relative percentage of Ki67-positive hepatocytes was increased in p53-deficient mice after NTBC withdrawal. Means ± SEM across multiple mice (n = 4–6). (*D*) NTBC withdrawal lead to markedly increased plasma levels of aspartate aminotransferase (AST) in the absence of p53. (*E*) p53-deficient mice retain their liver weight after 14 days of NTBC withdrawal. Means ± SEM (n = 6). (*F*) Immunoblots on total liver lysates from pooled samples (n = 4) to detect expression levels of the indicated cell-cycle–related proteins. (*G*) p21 levels were analyzed by quantitative polymerase chain reaction from *Fah*$^{-/-}$, *Fah/p21*$^{-/-}$, *Fah/p53*$^{-/-}$, and *Fah/Chk2*$^{-/-}$ mice treated with either 100% or 14 days with 0% NTBC. DDCT, delta-delta Ct; Gapdh, glyceraldehyde-3-phosphate dehydrogenase. *$P \leq .05$.

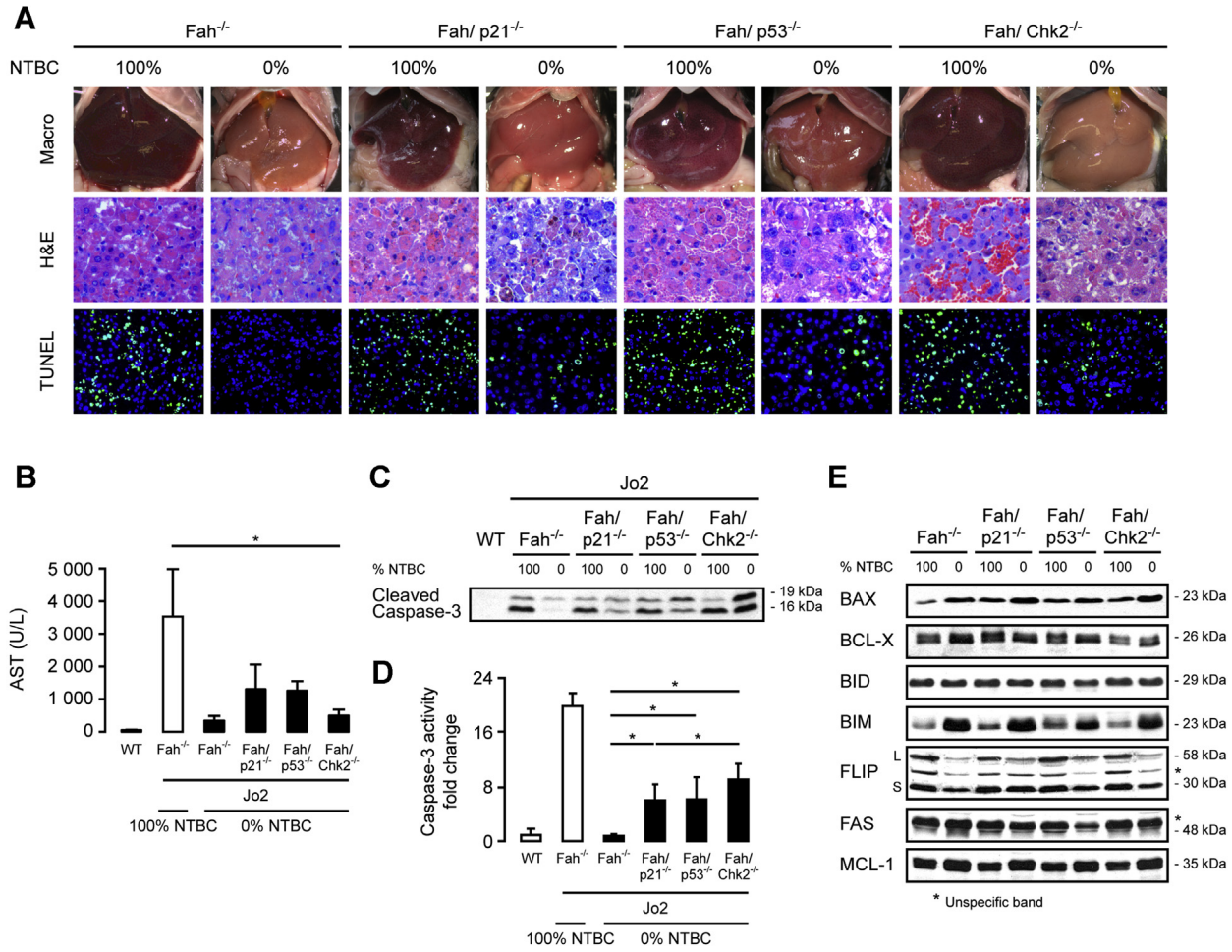

Figure 2. Apoptosis sensitivity was partially restored in *Chk2*, *p53*, and *p21*-deficient *Fah*$^{-/-}$ hepatocytes. (*A–E*) Eight-week-old *Fah*$^{-/-}$, *Fah/p21*$^{-/-}$, *Fah/p53*$^{-/-}$, and *Fah/Chk2*$^{-/-}$ mice on 100% NTBC treatment or 14 days after NTBC withdrawal were challenged with the anti-Fas antibody Jo2. (*A*) Representative macroscopic images of Fas-challenged animals, as well as H&E and TUNEL staining. *Fah/p21*$^{-/-}$, *Fah/p53*$^{-/-}$, and *Fah/Chk2*$^{-/-}$ mice show morphologic signs of aggravated liver damage and increased numbers of TUNEL-positive hepatocytes. (*B*) Plasma levels of aspartate aminotransferase (AST) as a surrogate marker for liver injury are increased in *Fah/p21*$^{-/-}$, *Fah/p53*$^{-/-}$, and *Fah/Chk2*$^{-/-}$ mice compared with *Fah*$^{-/-}$ mice off NTBC after Jo2 treatment, but do not reach the levels observed in *Fah*$^{-/-}$ mice on full NTBC supplementation (n = 3–5 per group, means ± SEM). Control: wild-type (WT) mice. (*C* and *D*) Jo2 treatment leads to increased cleaved caspase-3 expression (*C*, immunoblot on whole liver lysates) and (*D*) activity in *Fah/p21*$^{-/-}$, *Fah/p53*$^{-/-}$, and *Fah/Chk2*$^{-/-}$ off NTBC compared with *Fah*$^{-/-}$ controls (n = 3–6). Activity values were normalized against WT. Means ± SEM are shown. (*E*) Immunoblots to detect the levels of several pro-apoptotic and anti-apoptotic proteins in pooled liver lysates from *Fah*$^{-/-}$, *Fah/p21*$^{-/-}$, *Fah/p53*$^{-/-}$, and *Fah/Chk2*$^{-/-}$ mice on 100% NTBC and 14 days after NTBC withdrawal (n = 3–4). *$P \leq .05$. BAX, BCL2-associated X protein; BCL-X, B-cell lymphoma-extra large; BID, BH3 interacting domain death agonist; BIM, BCL2-like 11; FLIP, CASP8 and FADD-like apoptosis regulator; MCL-1, myeloid cell leukemia sequence 1.

serve as a physiologic protective mechanism in a situation of imminent liver failure. Apoptosis resistance, however, is reduced in *Fah/p21*$^{-/-}$ mice, implicating that p21 plays a role in the regulation of FAS-induced apoptosis in injured hepatocytes.[3] This observation raises the question whether protection from apoptosis is strictly dependent on the presence of p21, or whether CHK2 and p53 might exert similar effects on the apoptosis sensitivity of FAH-deficient hepatocytes.

To address this question, *Fah*$^{-/-}$, *Fah/p21*$^{-/-}$, *Fah/p53*$^{-/-}$, and *Fah/Chk2*$^{-/-}$ mice on 100% NTBC treatment or 14 days after NTBC withdrawal were challenged with the anti-FAS monoclonal antibody Jo2. After Jo2-mediated activation of the apoptotic machinery, microscopic examination of liver sections from *Fah*$^{-/-}$ mice on 100% NTBC showed pronounced hepatocyte destruction with massive hemorrhage and multiple TUNEL-positive hepatocytes, which was markedly suppressed in *Fah*$^{-/-}$ mice on 0% NTBC, in line with our previous report (Figure 2*A* and Sherr and Roberts[24]). In all double-knockout mice, including a *Fah/p21*$^{-/-}$ cohort, surrogate markers of liver damage (transaminase levels) and apoptosis (TUNEL-positive hepatocytes, cleaved caspase-3) were increased (Figure 2*A–D*) when compared with *Fah*$^{-/-}$ mice off NTBC, but the animals did not present

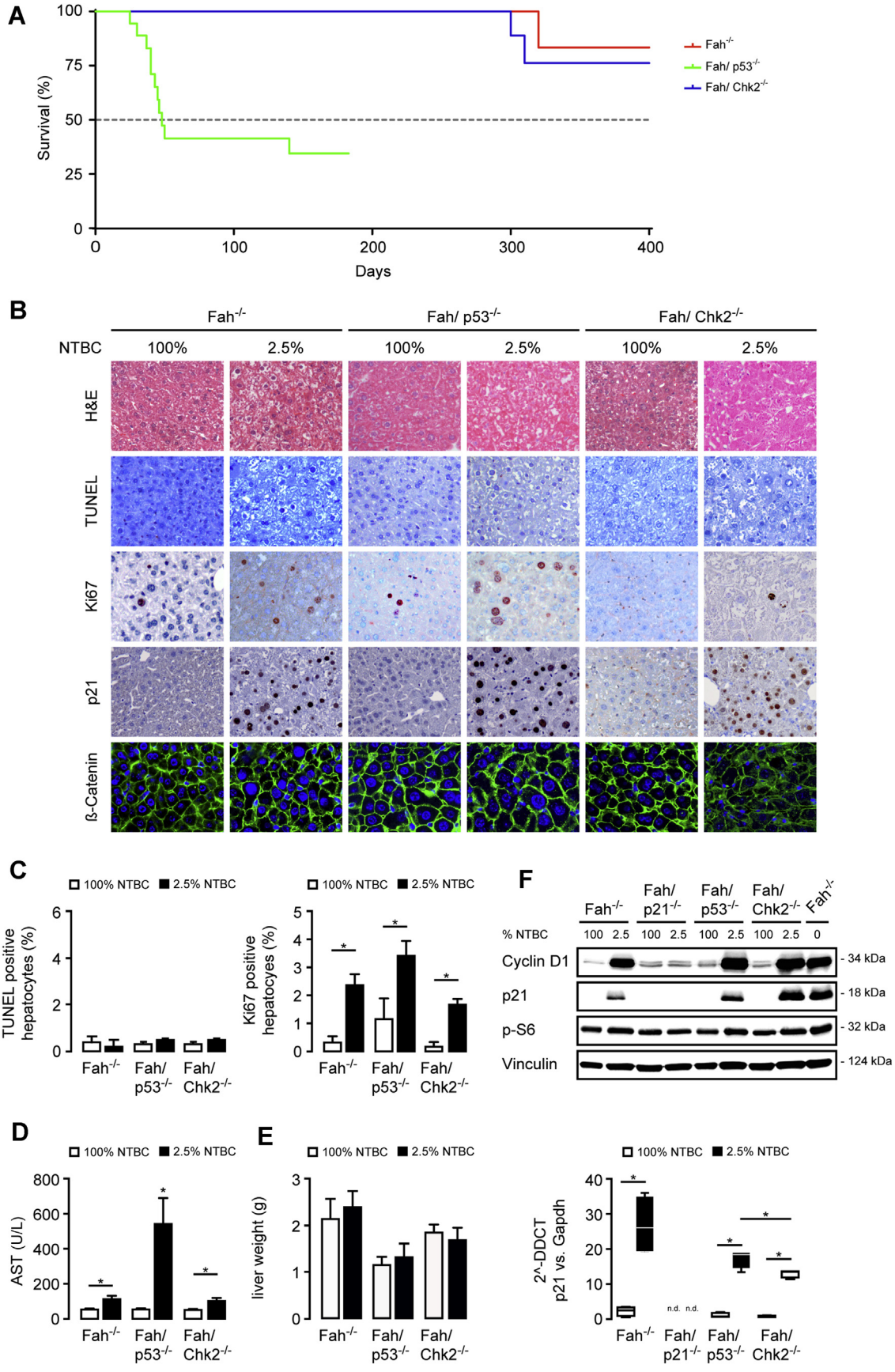
A
Survival (%)
Days
Fah-/-
Fah/ p53-/-
Fah/ Chk2-/-
B
NTBC
100%
2.5%
H&E
TUNEL
Ki67
p21
ß-Catenin
C
100% NTBC
2.5% NTBC
TUNEL positive hepatocytes (%)
Ki67 positive hepatocyes (%)
D
AST (U/L)
E
liver weight (g)
F
% NTBC
Cyclin D1
p21
p-S6
Vinculin
- 34 kDa
- 18 kDa
- 32 kDa
- 124 kDa
2^-DDCT p21 vs. Gapdh
n.d.

with the fulminant liver failure phenotype observed in Jo2-challenged Fah mice under 100% NTBC supplementation in the absence of concomitant injury. At this point, it is still enigmatic how apoptosis resistance is mediated in Fah-deficient hepatocytes in the context of liver injury.[25] Notably, loss of p21, p53, and CHK2 did not significantly alter the expression levels of pro-apoptotic or anti-apoptotic proteins such as B-cell lymphoma 2 (BCL2)-associated X protein, B-cell lymphoma-extra large, Bcl-2 homology 3 interacting domain death agonist, BCL2-like 11 (apoptosis facilitator), FADD-homologous ICE/CED-3-like protease-like inhibitory protein, myeloid cell leukemia 1, and FAS receptor in healthy or injured hepatocytes compared with *Fah*$^{-/-}$ controls (Figure 2*E*).

Together, these data indicate that the mechanisms that can protect hepatocytes from apoptosis in the context of liver injury remain at least partially intact in the absence of p53, p21, or CHK2. However, loss of either p53, p21, or CHK2 results in a shift toward an apoptosis phenotype.

p53 Is Essential for Survival of Fah-Deficient Mice With Moderate Chronic Liver Injury

The reaction of the liver to injury is highly context-dependent and influenced by the severity of the damaging insult. To analyze the role of p53 and CHK2 in an experimental setting of moderate long-term injury and to define their involvement in liver cancer formation, mice were exposed to a reduced treatment regimen of NTBC (2.5% of the normal dose) for up to 12 months. *Fah*$^{-/-}$ and *Fah/Chk2*$^{-/-}$ mice survived the low-dose NTBC treatment (Figure 3*A*). In contrast, the majority of *Fah/p53*$^{-/-}$ mice died, with a median overall survival of 48 days after NTBC reduction with some long-term survivors, indicating that the p53-regulated stress response is critically important for the survival of Fah-deficient mice during chronic liver injury (Figure 3*A*). Histologically, livers from *Fah*$^{-/-}$ and *Fah/Chk2*$^{-/-}$ mice on low-dose NTBC showed multiple abnormal hepatic features with mild acinar inflammation and prominent hepatocyte size variations (Figure 3*B*, H&E and β-catenin staining). In all groups, TUNEL-positive hepatocytes were scarce, further highlighting that apoptosis is not a predominant mechanism of cell death in FAA-induced acute and chronic liver injury (Figure 3*B* and *C*). Similar to the respective cohort off NTBC, aggravated biochemical and histologic liver injury also was evident in *Fah/p53*$^{-/-}$ mice on 2.5% NTBC (Figure 3*B* and *D*). In contrast to the profound cell-cycle arrest observed in Fah-deficient mice on 0% NTBC, several proliferating hepatocytes were found in livers of *Fah*$^{-/-}$ mice with moderate liver injury despite increased p21 levels (Ki67 staining) (Figure 3*B* and *C*). Further supporting the proliferative phenotype, cyclin D levels were increased in *Fah*$^{-/-}$, *Fah/p53*$^{-/-}$, and *Fah/Chk2*$^{-/-}$ mice (Figure 3*F* and Marhenke et al[26]), and there was no significant difference in liver weight between mice on and off NTBC (Figure 3*E*).

In contrast to the impaired regenerative response in *Fah/p21*$^{-/-}$ mice with moderate liver injury,[17] the percentage of proliferating hepatocytes was similar in *Fah*$^{-/-}$ mice with or without loss of *p53*$^{-/-}$ or *Chk2*$^{-/-}$. However, the increased hepatocyte proliferation was not sufficient to fully compensate the more severe liver injury and prevent the increased mortality in the majority of *Fah/p53*$^{-/-}$ mice, whereas the less pronounced injury in *Fah/Chk2*$^{-/-}$ mice allowed long-term survival similar to *Fah*$^{-/-}$ mice.

Loss of p53 Significantly Accelerates Tumor Development in Mice With Moderate Chronic Liver Injury

Liver tumor development can be critically influenced by predisposing genetic events, the degree of liver injury, and the proliferation rate, further complicated by the fact that these parameters frequently are interdependent. For instance, in *Fah/p21*$^{-/-}$ mice, tumor development correlated directly with the proliferative response and loss of p21 either accelerated or delayed tumorigenesis, depending on the severity of liver injury.[17]

Liver tumors were evident by macroscopic and histologic examination in less than half of *Fah*$^{-/-}$ mice (n = 10) after 6 months with a steady increase over time, reaching 76% after 9 months (n = 20) and 100% after 12 months (n = 20) (Figure 4*A* and *B*). In contrast to our observations in *Fah/p21*$^{-/-}$ mice, surviving *Fah/p53*$^{-/-}$ on 2.5% NTBC showed accelerated tumor development: the surviving *Fah/p53*$^{-/-}$ mice exhibited several large tumor foci with full penetrance and had to be killed at 6 months (n = 6) (Figure 4*A*, *B*, and *D*). Tumor incidence in *Fah/Chk2*$^{-/-}$ and *Fah*$^{-/-}$ mice was similar (n = 13) (Figure 4*B*), indicating that loss of CHK2 neither substantially accelerates tumorigenesis-like p53 deficiency nor delays tumorigenesis as previously observed in p21-deficient mice.[17] Of note, the tumor size was increased in *Fah/Chk2*$^{-/-}$ mice compared with *Fah*$^{-/-}$ mice after 9 (n = 12; $P \leq .05$) and 12 months (n = 11; $P \leq .05$) (Figure 4*C*).

Next, we addressed whether loss of p53 in the FAH context alters the chromosomal profile of resulting tumors.

Figure 3. (***See previous page***). **Loss of p53 aggravates liver injury and increases mortality in mice with moderate liver injury.** (*A*) Kaplan–Meier survival curves of *Fah*$^{-/-}$ (n = 15), *Fah/p53*$^{-/-}$ (n = 15), and *Fah/Chk2*$^{-/-}$ (n = 15) mice on 2.5% NTBC treatment. (*B–E*) *Fah*$^{-/-}$, *Fah/p53*$^{-/-}$, and *Fah/Chk2*$^{-/-}$ mice 4 weeks on 2.5% NTBC compared with the respective 100% NTBC controls. (*B*) Representative H&E, immunohistochemistry, and immunofluorescence images as indicated. (*C*) *Left*: The relative percentage of TUNEL-positive hepatocytes was not significantly different between the genotypes. Means ± SEM across multiple mice (n = 4–6). *Right*: The relative percentage of Ki67-positive hepatocytes was increased after NTBC reduction. Means ± SEM across multiple mice (n = 4–6). (*D*) NTBC reduction lead to markedly increased plasma levels of aspartate aminotransferase (AST) in the absence of p53. (*E*) Liver weight was retained in all mice after 14 days of NTBC reduction. Means ± SEM (n = 4–6). (*F*) *Upper*: Immunoblots on total liver lysates from pooled samples (n = 4) for key cell-cycle–related proteins. *Lower*: p21 levels were analyzed by quantitative polymerase chain reaction from *Fah*$^{-/-}$, *Fah/p21*$^{-/-}$, *Fah/p53*$^{-/-}$, and *Fah/Chk2*$^{-/-}$ mice treated with either 100% or 4 weeks on 2.5% NTBC. **P* ≤ .05. DDCT, delta-delta Ct; Gapdh, glyceraldehyde-3-phosphate dehydrogenase.

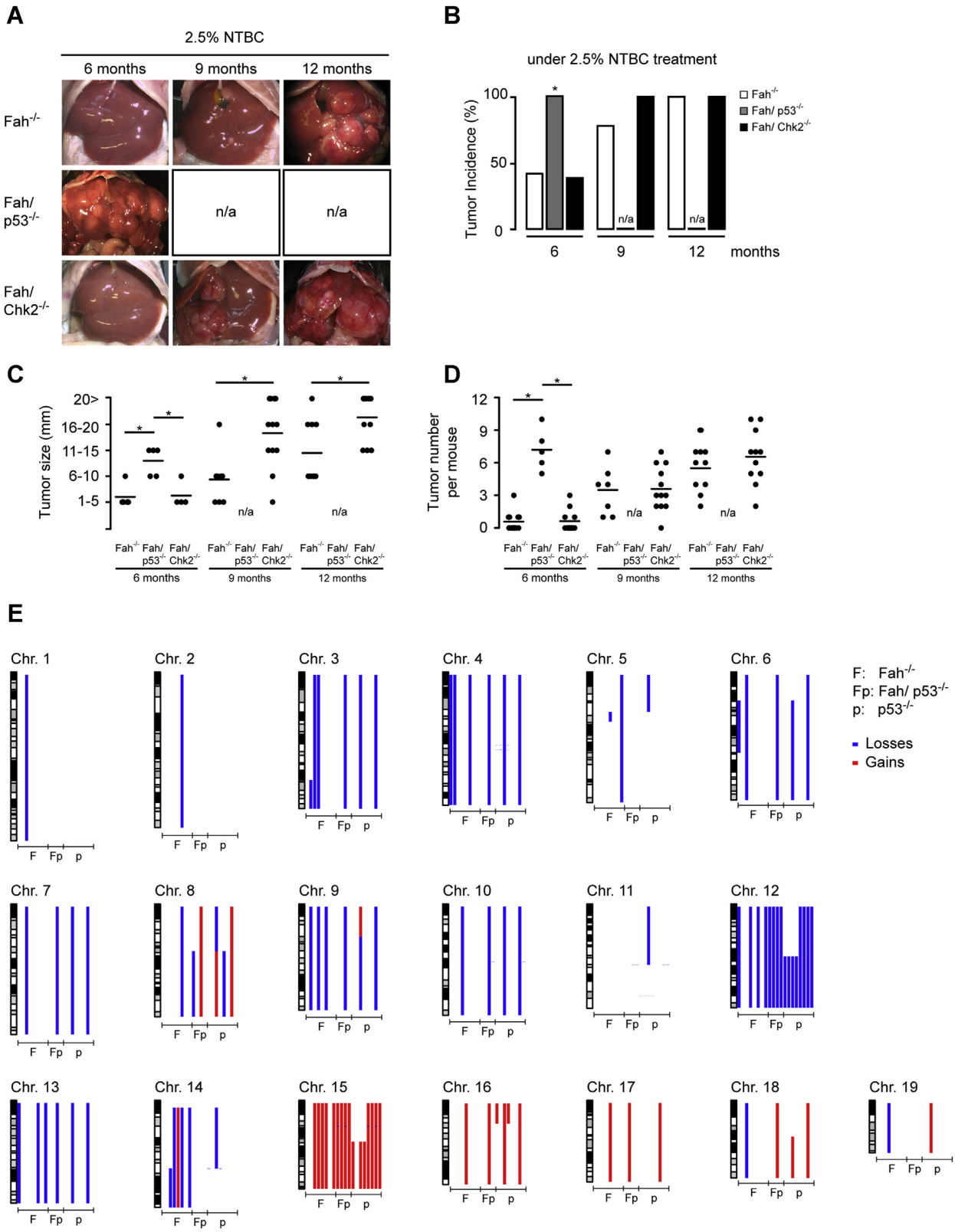

Figure 4. Loss of p53 accelerates tumor development but does not increase chromosomal instability in FAA-induced tumors. (*A–D*) *Fah*$^{-/-}$, *Fah/p53*$^{-/-}$, and *Fah/Chk2*$^{-/-}$ mice received either 100% or 2.5% NTBC for 6, 9, and 12 months. (*A* and *B*) Loss of p53 accelerated liver tumor formation in Fah-deficient mice. (*C* and *D*) Size and tumor numbers at the indicated time points. Each *dot* represents the maximum value measured per mouse, *lines* indicate the mean value. (*E*) aCGH on liver tumors from *Fah*$^{-/-}$ (F) and *Fah/p53*$^{-/-}$ (Fp) mice on 2.5% NTBC shows numerous chromosomal aberrations. Tumors from *p53*$^{-/-}$ mice were included as controls (p). *$P \leq .05$. n/a, not available.

Table 1. Classification of Hallmark Gene Sets

Classes	Hallmark gene sets	Genes, n
p53/DNA damage response	HALLMARK_p53_PATHWAY HALLMARK_DNA_REPAIR	282
Oxidative stress	HALLMARK_XENOBIOTIC_METABOLISM HALLMARK_REACTIVE_OXIGEN_SPECIES_PATHWAY HALLMARK_HEME_METABOLISM HALLMARK_BILE_ACID_METABOLISM	614
Inflammation	HALLMARK_INTERFERON_GAMMA_RESPONSE HALLMARK_INFLAMMATORY_RESPONSE HALLMARK_ALLOGRAFT_REJECTION HALLMARK_TNFa SIGNALING VIA NFKB HALLMARK_IL6, JAK, STAT3 SIGNALING	508
Proliferation	HALLMARK_PI3K_AKT_MTOR_SIGNALING HALLMARK_MTORC1_SIGNALING HALLMARK_WNT_BETA_CATENIN_SIGNALING HALLMARK_G2M_CHECKPOINT HALLMARK_MYC_TARGETS_V2 HALLMARK_MYC_TARGETS_V1 HALLMARK_E2F_TARGETS HALLMARK_MITOTIC_SPINDLE	791

Array comparative genomic hybridization (aCGH) was performed on liver tumors dissected from *Fah*$^{-/-}$ and *Fah/p53*$^{-/-}$ mice, and we included a control group of tumors that arose in *p53*$^{-/-}$ mice. Chromosomal gains and losses were evident in all liver tumors examined (*Fah*$^{-/-}$, n = 8; *Fah/p53*$^{-/-}$, n = 4; *p53*$^{-/-}$, n = 8) (Figure 4*E*). A recurring chromosomal event across all genotypes was a copy number gain of chromosome 15, overlapping the *c-Myc* locus, which also is amplified frequently in human hepatocellular carcinoma (syntenic region on chromosome 8). In addition, chromosomal losses on chromosome 12 occurred in most p53-deficient tumors. Overall, aCGH did not show a striking increase in genomic instability in p53-deficient vs p53-proficient tumors.

In summary, loss of p53 not only dramatically increases liver injury and mortality of Fah-deficient mice, but also significantly accelerates tumor development in the liver, thereby confirming the strong tumor-suppressive role of p53. In contrast to the accelerated tumor development in p53-deficient mice and the delayed tumorigenesis in p21-deficient mice, loss of CHK2 did not significantly modulate tumor occurrence in the Fah model.

Gene Expression Profiles Are Dominated by the Severity of Liver Injury, But Also Reflect p53-Dependent Effects on Proliferation and Oxidative Stress Response

Thus far, our focused approaches did not show phenotype-specific differences in signaling pathway activation (Figures 1*F* and 3*F*). To better understand how loss of p53 modulates the cellular stress response, and to identify gene expression profiles that are associated with liver injury, regeneration, survival, and tumor development, we performed microarray analysis on reverse-transcribed RNA extracted from *Fah*$^{-/-}$ and *Fah/p53*$^{-/-}$ mice with moderate (3 months on 2.5% NTBC, n = 4) or severe liver injury (0% NTBC for 2 weeks, n = 4), and their respective controls (100% NTBC, n = 4). In addition, based on our observation that loss of p53 under 0% NTBC was not sufficient to recapitulate the prolonged overall survival of Fah-deficient mice lacking p21 expression, we included samples from the *Fah/p21*$^{-/-}$ cohort (n = 4) to directly compare how loss of p21 vs p53 affects the adaptive response in *Fah*$^{-/-}$ mice with severe liver injury.

Gene set enrichment analysis (GSEA) using the 50 hallmark gene sets derived from the Molecular Signature Database was performed to identify relevant biological processes.[27] First, transcriptional profiles from mice with moderate and severe liver injury were compared with profiles from the corresponding healthy controls. Several significantly enriched gene sets were identified, and the majority of these gene sets were allocated to 4 main classes: p53/DNA damage response, oxidative stress response, inflammation, and proliferation (Table 1). Overall, these gene sets thematically recapitulate our previous observations on the role of p21,[3,17] mechanistic target of rapamycin kinase,[19] and nuclear factor erythroid 2-related factor 2 (NRF2)[20] in the *Fah*$^{-/-}$ model.

As expected, the p53/DNA damage response class segregated with liver injury in p53-proficient mice when compared with their 100% counterparts (Figure 5*A*, green). Of note, this class also was enriched in p53-deficient mice compared with healthy double-knockout mice (Figure 5*B*), indicating that a subset of genes in the p53 pathway gene set can be regulated independently of p53 during liver injury. On the contrary, when comparing different genotypes, the p53/DNA damage response class was enriched in p53-proficient mice compared with p53-deficient mice,

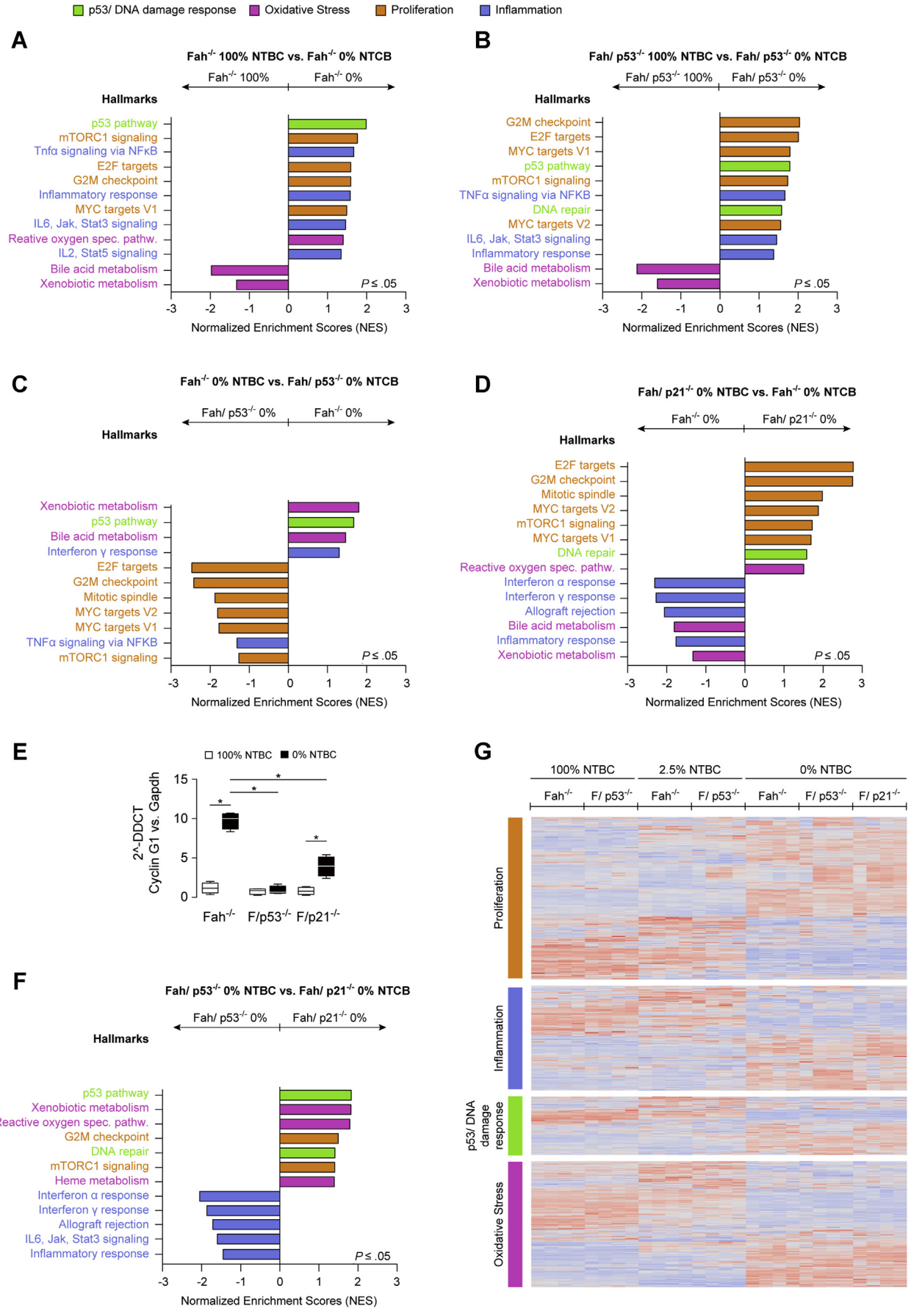
p53/ DNA damage response
Oxidative Stress
Proliferation
Inflammation
A
Fah-/- 100% NTBC vs. Fah-/- 0% NTCB
Fah-/- 100%
Fah-/- 0%
Hallmarks
p53 pathway
mTORC1 signaling
Tnfα signaling via NFκB
E2F targets
G2M checkpoint
Inflammatory response
MYC targets V1
IL6, Jak, Stat3 signaling
Reative oxygen spec. pathw.
IL2, Stat5 signaling
Bile acid metabolism
Xenobiotic metabolism
P ≤ .05
Normalized Enrichment Scores (NES)
B
Fah/ p53-/- 100% NTBC vs. Fah/ p53-/- 0% NTCB
Fah/ p53-/- 100%
Fah/ p53-/- 0%
Hallmarks
G2M checkpoint
E2F targets
MYC targets V1
p53 pathway
mTORC1 signaling
TNFα signaling via NFKB
DNA repair
MYC targets V2
IL6, Jak, Stat3 signaling
Inflammatory response
Bile acid metabolism
Xenobiotic metabolism
P ≤ .05
Normalized Enrichment Scores (NES)
C
Fah-/- 0% NTBC vs. Fah/ p53-/- 0% NTCB
Fah/ p53-/- 0%
Fah-/- 0%
Hallmarks
Xenobiotic metabolism
p53 pathway
Bile acid metabolism
Interferon γ response
E2F targets
G2M checkpoint
Mitotic spindle
MYC targets V2
MYC targets V1
TNFα signaling via NFKB
mTORC1 signaling
P ≤ .05
Normalized Enrichment Scores (NES)
D
Fah/ p21-/- 0% NTBC vs. Fah-/- 0% NTCB
Fah-/- 0%
Fah/ p21-/- 0%
Hallmarks
E2F targets
G2M checkpoint
Mitotic spindle
MYC targets V2
mTORC1 signaling
MYC targets V1
DNA repair
Reactive oxygen spec. pathw.
Interferon α response
Interferon γ response
Allograft rejection
Bile acid metabolism
Inflammatory response
Xenobiotic metabolism
P ≤ .05
Normalized Enrichment Scores (NES)
E
100% NTBC
0% NTBC
2^-DDCT Cyclin G1 vs. Gapdh
Fah-/-
F/p53-/-
F/p21-/-
F
Fah/ p53-/- 0% NTBC vs. Fah/ p21-/- 0% NTCB
Fah/ p53-/- 0%
Fah/ p21-/- 0%
Hallmarks
p53 pathway
Xenobiotic metabolism
Reactive oxygen spec. pathw.
G2M checkpoint
DNA repair
mTORC1 signaling
Heme metabolism
Interferon α response
Interferon γ response
Allograft rejection
IL6, Jak, Stat3 signaling
Inflammatory response
P ≤ .05
Normalized Enrichment Scores (NES)
G
100% NTBC
2.5% NTBC
0% NTBC
Fah-/-
F/ p53-/-
Fah-/-
F/ p53-/-
Fah-/-
F/ p53-/-
F/ p21-/-
Proliferation
Inflammation
p53/ DNA damage response
Oxidative Stress

which validates the dependency of these gene sets on the presence of intact p53 (Figure 5*C*).

Gene sets assigned to the proliferation class were enriched significantly in severe injury conditions (Figure 5*A* and *C*, orange) in both p53-proficient and p53-deficient mice compared with the respective healthy controls. When comparing mice with liver injury, proliferation gene sets were enriched in the absence of p53 (Figure 5*C*) and p21 (Figure 5*D*). Next, we specifically analyzed the proliferation class for differentially regulated genes that segregated with the p53 status. Among the 791 genes included in the proliferation class, 190 genes were significantly differentially regulated between *Fah*$^{-/-}$ and *Fah/p53*$^{-/-}$ mice, but only 3 genes (epidermal growth factor receptor, cyclin G1, asparagine synthetase) were more than 2-fold up-regulated in *Fah* $^{-/-}$ mice compared with *Fah/p53*$^{-/-}$ mice. Of these 3 genes, cyclin G1 has been described previously as a p53-dependent cell-cycle inhibitor in hepatocytes, and increased levels of cyclin G1 were confirmed in *Fah*$^{-/-}$ mice with severe liver injury, although they were significantly lower in *Fah/p53*$^{-/-}$ and *Fah/p21*$^{-/-}$ mice (Figure 5*E*), indicating that cyclin G1 might contribute to the cell-cycle arrest in *Fah*$^{-/-}$ mice with severe liver injury.

Oxidative stress response–related gene sets include a broad array of genes that are either induced or suppressed to counteract increased oxidative stress after NTBC reduction. In agreement with our previous findings, gene sets included in the category of oxidative stress response were differently regulated in *Fah*$^{-/-}$ mice with severe liver injury (Figure 5*A*). Aggravated liver injury and high mortality of *Fah/p53*$^{-/-}$ mice was accompanied by an impaired oxidative stress response after NTBC withdrawal compared with the p53-proficient *Fah*$^{-/-}$ mice (Figure 5*C*). The oxidative stress response class also was differentially regulated between *Fah/p53*$^{-/-}$ and *Fah/p21*$^{-/-}$ mice, which likely contributes to the more severe liver injury and high mortality of *Fah/p53*$^{-/-}$ mice compared with *Fah/p21*$^{-/-}$ mice taken off NTBC despite the high hepatocyte proliferation rate in both genotypes (Figure 5*F*).

Despite the experimental evidence that *Fah*$^{-/-}$ mice respond differently to injury depending on the presence or absence of p53 or p21, it should be noted that the global gene expression patterns, and also the regulation within the hallmark gene sets, were influenced most prominently by the degree of liver injury and less affected by the genotype of the respective genetic groups (Figure 5*G*).

Together, the comprehensive GSEA confirmed the strong activation of the p53 pathway and an oxidative stress response in the Fah model. The gene set class proliferation was induced in *Fah/p53*$^{-/-}$ and *Fah/p21*$^{-/-}$ mice. Moreover, increased liver injury and high mortality of *Fah/p53*$^{-/-}$ mice occurred despite a compensatory induction of p53-related genes and was accompanied by an impaired oxidative stress response after NTBC reduction and withdrawal.

p21 Fails to Inhibit Retinoblastoma Phosphorylation in Fah/p53$^{-/-}$ *Mice*

The gene expression analysis confirmed a strong induction of proliferation-related genes in *Fah/p53*$^{-/-}$ mice with severe liver injury occurred despite the p21 expression (Figure 1*F*). D-type cyclins and the kinases cyclin-dependent kinase (CDK)4 and CDK6 regulate G0–G1–S progression by contributing to the phosphorylation and subsequent inactivation of the retinoblastoma (RB) gene product. Assembly of active cyclin D–CDK complexes in response to mitogenic signals is regulated negatively by the cyclin-dependent kinase inhibitors p21 and p27. On the other hand, a non-catalytic function of cyclin D–dependent kinases is the sequestration of p21 and Cyclin-dependent kinase inhibitor 1B (p27) during the G1 phase to relieve cyclin E–CDK2 from their constraint, thereby facilitating its activation later in the G1 phase.[24] To understand whether the unexpected finding that p21 failed to inhibit RB phosphorylation and cell-cycle progression in *Fah/p53*$^{-/-}$ mice results from an impaired cyclin/CDK/cyclin-dependent kinase inhibitor complex formation, we performed immunoprecipitation (IP) of the individual components of the complex. IP with an antibody against p21 showed that p21 associated with cyclin D1, CDK4, and also with CDK2 in *Fah/p53*$^{-/-}$ and in *Fah* $^{-/-}$ mice (Figure 6*A*). The interaction of cyclin D1/CDK4 and p21 was confirmed by IP of cyclin D1. Similarly, IP with an anti-p27 antibody showed an interaction of p27 with cyclin D1 and CDK4 in both *Fah/p53*$^{-/-}$ and in *Fah* $^{-/-}$ mice. In line with the strong regenerative response, RB was phosphorylated only in *Fah/p53*$^{-/-}$ mice and *Fah/p21*$^{-/-}$ mice, but not in *Fah* $^{-/-}$ mice with severe liver injury (Figure 6*B*).

Together, these data indicate that the interaction of p21 with cyclin D1, CDK4, and CDK2, and the interaction of p27 with cyclin D1 and CDK4, is not impaired in *Fah/p53*$^{-/-}$ mice. In contrast to *Fah*$^{-/-}$ mice, this interaction, however, fails to inhibit RB phosphorylation and cell-cycle progression of hepatocytes during liver injury.

Fah/p53$^{-/-}$ *Mice Show an Impaired Oxidative Stress Response*

The gene expression analysis suggests that an impaired oxidative stress response contributes to the high mortality of *Fah/p53*$^{-/-}$ mice. FAA is a highly electrophilic compound that induces DNA damage and oxidative stress in vitro and in vivo.[28] In line with these studies, we previously showed

Figure 5. (***See previous page***). **Gene expression profiling in p53-proficient and p53-deficient mice with moderate and severe liver injury.** (*A–D* and *F*) Normalized Enrichment Scores (NES) of hallmark gene sets stratified into the categories p53/DNA damage response, oxidative stress, proliferation, and inflammation. (*E*) Quantitative polymerase chain reaction (PCR) analysis shows that *p53* deficient *Fah*$^{-/-}$ mice off NTBC lack the decisive transcriptional up-regulation of cyclin G1. (*G*) Gene expression patterns are prominently influenced by the type of liver injury and less affected by the different genotypes. DDCT, delta-delta Ct; Gapdh, glyceraldehyde-3-phosphate dehydrogenase; G2M, G2/M-phase; IL, interleukin; Jak, Janus kinase; mTorc1, mTOR complex 1; MYC, myelocytomatosis oncogene; NFKB, nuclear factor κB; Stat3, signal transducer and activator of transcription 3; TNF, tumor necrosis factor.

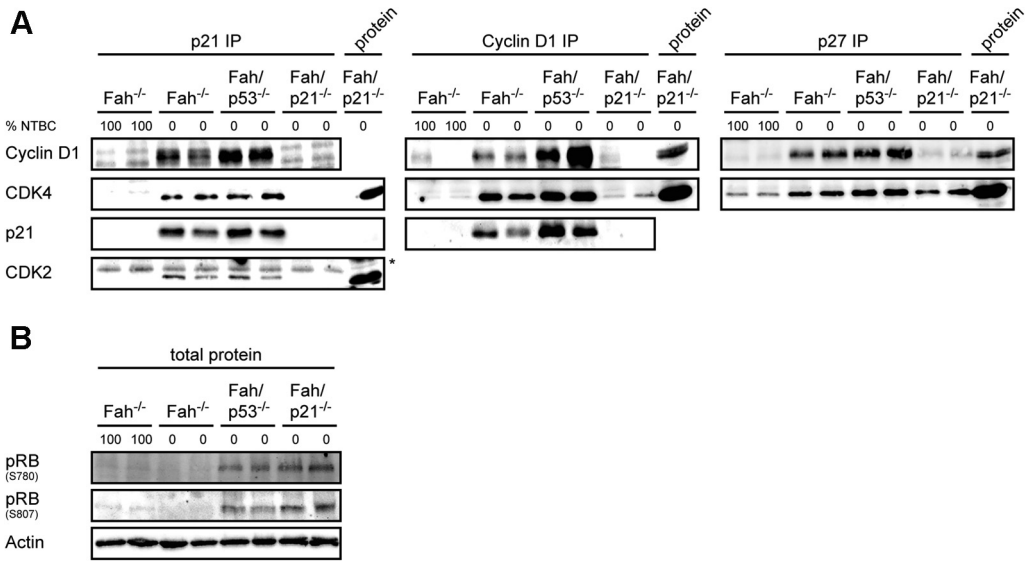

Figure 6. Formation of cyclin/CDK/cyclin-dependent kinase inhibitor (CKI) complexes during liver injury. (*A*) Extracts from liver tissue were subjected to immunoprecipitation and Western analysis. Association of p21 with cyclin D1, CDK4, and CDK2; association of cyclin D1 with CDK4 and p21; association of p27 with cyclin D1 and CDK4. (*B*) Immunoblots on total liver lysates from 2 samples of each group for phospho-RB (pRB) were performed.

that the NRF2-mediated anti-oxidative stress response is critically important for the survival of *Fah*-deficient mice,[20] and a strong induction of NRF2 target genes such as reduced nicotinamide adenine dinucleotide phosphate dehydrogenase, quinone 1 and heme oxygenase 1 was evident in *Fah*$^{-/-}$ and *Fah/p53*$^{-/-}$ mice (Figure 7*A* and *C*).

Accumulation of electrophilic compounds is counterbalanced by changes in antioxidants such as glutathione (GSH). Previously, it has been shown that acute FAA accumulation leads to a depletion of GSH in vivo,[20] which enhances FAA-induced cell death and also amplifies its mutagenicity.[29] The biosynthesis of glutathione is dependent on the availability of the cystine/glutamate transporter (solute carrier family 7 [cationic amino acid transporter, y+ system], member 11), a member of heterodimeric sodium-dependent amino acid transporter that imports cystine and exports glutamate, and of a glutamate-cysteine ligase, which consists of a heavy catalytic subunit (glutamate cysteine ligase, catalytic subunit) and a light regulatory subunit (glutamate cysteine ligase, modifier subunit). Electrophilic compounds and products of oxidative stress subsequently are detoxified by conjugation with glutathione by enzymes such as glutathione S-transferase mu4. In agreement with our previous observation,[20] *Gclc*, *Gstm4*, and *Slc7a11* were strongly induced in *Fah*$^{-/-}$ mice after NTBC reduction, whereas they were significantly lower in p53-deficient livers (Figure 7*A* and *C*). In line with the compensatory increase in GSH production upon liver injury, GSH levels were increased in both groups on 2.5% NTBC (Figure 7*B*). However, glutathione disulfide (GSSG) as the oxidized form of GSH was increased exclusively in liver lysates of *Fah/p53*$^{-/-}$ mice, leading to an increased GSSG:GSH ratio suggestive of a net shift toward insufficient compensation (Figure 7*B*).

Together, accumulation of FAA leads to a strong oxidative stress response in the liver, which is impaired in *Fah/p53*$^{-/-}$ mice. Notably, loss of p53 could not be compensated by other regulators of the oxidative stress response such as NRF2, suggesting that a coordinated expression of cytoprotective p53 target genes is critically important to protect Fah-deficient mice against FAA-induced liver injury.

Discussion

p53 is embedded in an intricate network of upstream regulators and downstream effectors that, in a concerted action, determine how a cell responds to damage. This response is highly flexible and context-dependent, and despite extensive efforts, a universal set of p53 target genes has not yet been defined.[5] In the Fah model, loss of p53 severely aggravated liver injury and increased mortality. Overall, the phenotype of *Fah/p53*$^{-/-}$ mice was reminiscent of our previous observations in *Fah*$^{-/-}$ mice with targeted deletion of *Nrf2*.[20] Both p53 and NRF2 play a fundamental role in maintaining the redox homeostasis of hepatocytes by controlling the expression of key components of the glutathione and thioredoxin antioxidant system, as well as enzymes involved in reduced nicotinamide adenine dinucleotide phosphate regeneration and xenobiotic detoxification. Compared with *Fah*$^{-/-}$ controls, the GSSG:GSH ratio was increased significantly in *Fah/p53*$^{-/-}$ mice as a consequence of the insufficient ability of hepatocytes to compensate the FAA-induced oxidative stress. Nevertheless, the antioxidant N-acetylcysteine alone was not sufficient to relieve the increased liver injury in *Fah/p53*$^{-/-}$ mice (data not shown) or in *Fah/Nrf2*$^{-/-}$ mice.[20] Thus, our data suggest that both a coordinate p53- and NRF2-regulated anti-

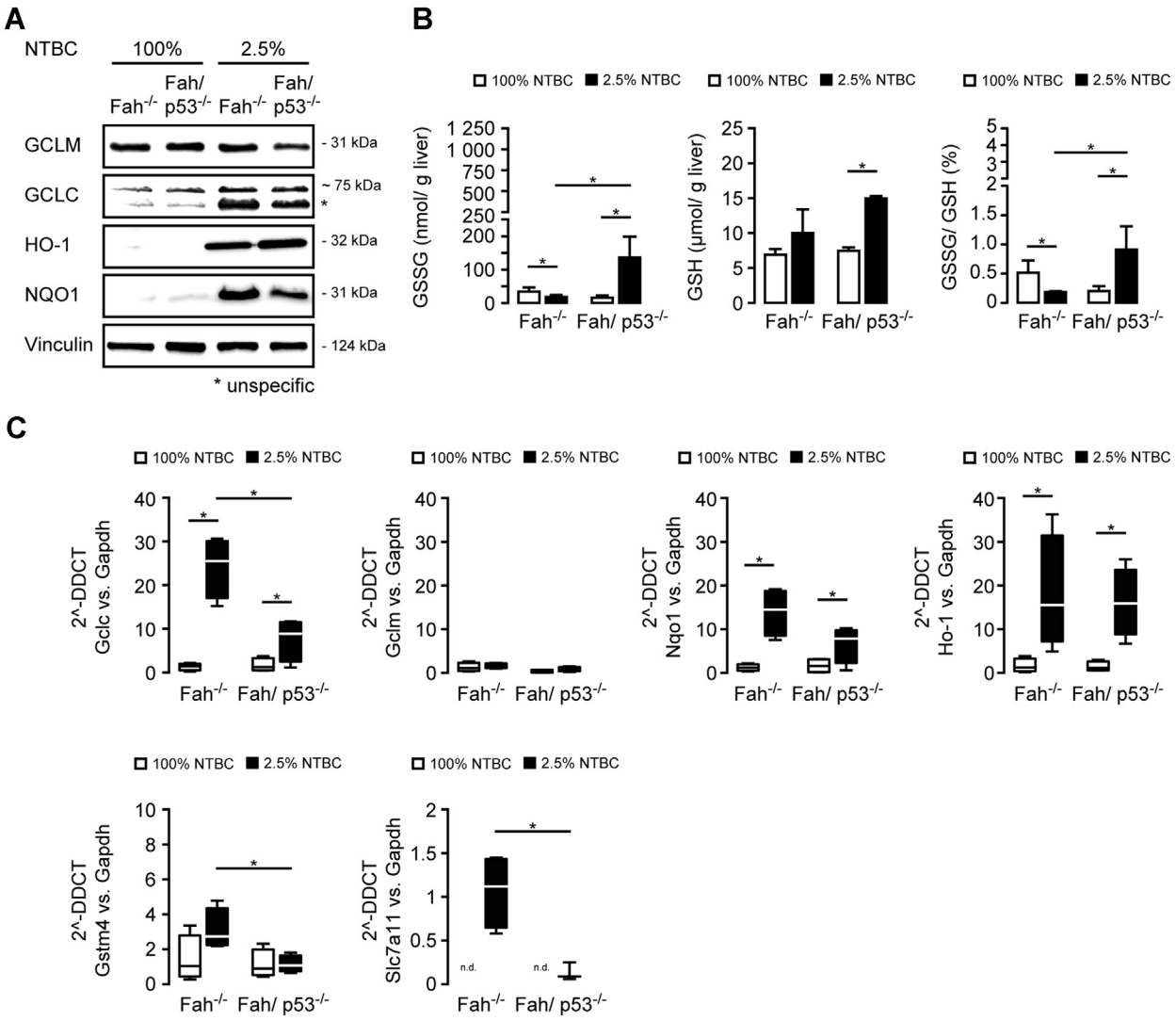

Figure 7. *Fah/p53*$^{-/-}$ mice show an impaired oxidative stress response. (*A–E*) *Fah*$^{-/-}$ and *Fah/p53*$^{-/-}$ mice were treated with 100% or 2.5% NTBC for 4 weeks. (*A*) Immunoblot on pooled liver samples (n = 4) for key regulators of the oxidative stress response. (*B*) GSSG/GSH ratio shows an impaired oxidative stress response in *Fah/p53*$^{-/-}$ mice. (*C*) Quantitative polymerase chain reaction (PCR) confirms significantly lower levels of selected members of the anti-oxidative stress response (*Gclc*, *Gstm4*, and *Slc7a11*) in *p53*-deficient *Fah*$^{-/-}$ mice. Medians in box-and-whisker plots (Tukey test). *$P \leq .05$. DDCT, delta-delta Ct; Gapdh, glyceraldehyde-3-phosphate dehydrogenase; Gclc, glutamate-cysteine ligase, catalytic subunit; Gclm, glutamate-cysteine ligase, modifier subunit; HO-1, heme oxygenase 1; n.d., not detectable; NQO1, NAD(P)H dehydrogenase, quinone 1.

oxidative stress response is required to protect hepatocytes from injury.

The liver has a remarkable ability to regenerate, and both moderate and severe liver damage upon NTBC reduction was associated with increased proliferation in the absence of p53. However, the proliferative response in p53-deficient mice on low-dose NTBC was not sufficient to prevent early mortality. In contrast, mice with severe acute injury (0% NTBC) were capable of mounting a compensatory proliferative response that rescued them from accelerated death. However, the delivery of an additional insult to the p53-deficient liver through partial hepatectomy tipped the delicate balance toward liver failure.

Several previous studies have delineated the critical involvement of p21 as one of the pivotal p53 target genes in liver regeneration, and we have shown that p21 induces a profound cell-cycle arrest in *Fah*-deficient mice with severe liver injury.[17] Unexpectedly, the strong induction of p21 is not dependent on p53 or on its upstream regulator CHK2. Moreover, the p53-independent p21 induction is not able to prevent hepatocyte proliferation, indicating that p21 is necessary but not sufficient to inhibit cell-cycle progression in the liver.

Activation of established pathways that regulate liver regeneration was evident in all mice with liver injury, but did not correlate with the proliferative capabilities of the different cohorts. Of note, the physical interaction of p21 with cyclin D1, CDK4, and CDK2 was not impaired in *Fah/p53*$^{-/-}$ mice, but failed to inhibit phosphorylation of RB. On the molecular level, NTBC withdrawal led to a strong

induction of genes associated with proliferation, irrespective of the genotype-dependent phenotypes. Among these genes, transcriptional regulation of cyclin G1 correlated with the proliferative response in *Fah*$^{-/-}$ and *Fah/p53*$^{-/-}$ mice. Cyclin G1 was identified previously as a p53 target gene that not only regulates stabilization of p53 by promoting protein degradation through Mouse double minute 2 homolog phosphorylation, but also acts as a cell-cycle checkpoint in hepatocytes.[30–32] Thus, cell-cycle progression in the absence of p53 might be facilitated in part by low levels of cyclin G1, but additional studies are necessary to unravel the molecular mechanism why p21 fails to inhibit hepatocyte proliferation in the absence of p53 during chronic liver injury.

p53-/p21-mediated cell-cycle arrest in Fah mice is accompanied by a resistance to apoptosis, reminiscent of a senescence phenotype.[33,34] Notably, although loss of either p21 or p53 restored hepatocyte proliferation, apoptosis resistance was relieved only partially in *Fah/p21*$^{-/-}$, *Fah/p53*$^{-/-}$, and *Fah/Chk2*$^{-/-}$ mice challenged with the FAS antibody Jo2. This suggests that the apoptosis resistance of *Fah*$^{-/-}$ mice cannot be fully attributed to p53-/p21-mediated senescence.

One potential limitation of our study could be the choice of a conditional liver-specific p53 knockout in contrast to the constitutive and ubiquitous loss of gene expression in *p21*$^{-/-}$ and *Chk2*$^{-/-}$ knockout mice. The conditional p53 allele was chosen because of the early tumor incidence in *p53*$^{-/-}$ mice (mainly lymphomas and sarcomas), whereas *p21*$^{-/-}$ and *Chk2*$^{-/-}$ knockout mice do not have an overt phenotype. Moreover, tyrosine metabolism occurs only in hepatocytes and proximal renal tubular cells, leading to FAA-induced injury specifically in these 2 organs. We therefore do not envision that loss of p21 or CHK2 in nonparenchymal cells has a major impact on the observed phenotypes.

In summary, we show that, in a model of metabolic liver injury, loss of *p53*, but not of *Chk2*, impairs the oxidative stress response and aggravates liver damage, indicating that, beyond its role as a tumor suppressor, intact p53 exerts an immediate protective effect on hepatocytes.

The increased regenerative potential in the absence of p53 is only partially capable of compensating the surplus injury and not sufficient to promote survival. Our work highlights that, although gene expression patterns are dominated by the severity of the damaging insult, characteristic phenotypes are created through genetic abrogation of individual components of the multilevel cascade that controls cell-cycle progression. The extent to which loss of gene function can be compensated, or affects liver injury and proliferation, is related to the level at which the cascade is interrupted. Although loss of the upstream regulator *Chk2* is dispensable in the model, cell-cycle control during chronic liver injury critically depends on the presence of both p53 and its downstream effector p21. Our work shows a complex interdependency between p21 and p53: neither the p53-independent induction of p21 nor activation of p53 in the absence of p21 is sufficient to prevent hepatocyte proliferation. Although loss of either p53 or p21 can elicit a strong proliferative response, only loss of p53 leads to increased liver injury and mortality, which cannot be compensated by increased liver regeneration.

Thus, damaging insults to the liver activate complex and interwoven response programs, whose net result is determined by the susceptibility to the damaging agent and the ability to regenerate. The type and the degree of injury, but also the underlying genetic landscape of the organism, are key modifiers of the injury response and can produce distinct, or even opposite, phenotypical outcomes.

Materials and Methods

Animal Experiments

All animal experiments were approved by local authorities (Lower Saxony State Office for Consumer Protection and Food Safety). The B6;129-Fah^{tm1Mgo} (*Fah*$^{-/-}$)[35] mice were crossed to the C57BL/6J-Tg(Alb1-cre)7Gsc-FVB.129-Trp53^{tm1Brn} (*p53*$^{fl/fl}$*/Alfp-Cre*+), C57BL/6-Cdkn1a^{tm1Ty1}/J (*p21*$^{-/-}$), and C57BL/6-Chk2^{tm1Mak} (*Chk2*$^{-/-}$) strain for several generations to generate Fah^{tm1Mgo}-C57BL/6J-Tg(Alb1-cre)7Gsc-FVB.129-Trp53^{tm1Brn} (*Fah*$^{-/-}$*/p53*$^{fl/fl}$*/Alfp-Cre*, ie, *Fah/p53*$^{-/-}$), B6;129-Fah^{tm1Mgo}-C57BL/6-Cdkn1a^{tm1Ty1}/J (*Fah/p21*$^{-/-}$), and C57BL/6-Fah^{tm1Mgo}-C57BL/6-Chk2^{tm1Mak} (*Fah/Chk2*$^{-/-}$) double-knockout mice. Drinking water was supplemented with 7.5 mg/L NTBC[18] unless otherwise indicated, and mice had access to food (Altromin1324 M; Altromin, Lage, Germany) and water ad libitum. Mice were housed in individually ventilated cages and all experiments were performed during the daytime of a 14-/10-hour day/night cycle. Kaplan–Meier survival curves were generated after NTBC reduction (2.5%) or withdrawal (0%) as previously published.[21] Tumor incidence (including size and number) were evaluated for all genotypes at the same time, data from *Fah*$^{-/-}$ (included in Figure 4) and *Fah/p21*$^{-/-}$ mice were reported previously.[17]

DNA Microarray Hybridization and Analysis

The quality and integrity of the total RNA were analyzed on an Agilent Technologies 2100 Bioanalyzer (Agilent Technologies, Santa Clara, CA). A total of 500 ng total RNA was applied for Cy3-labeling reaction using the 1-color Quick Amp Labeling protocol (Agilent Technologies). Labeled complementary RNA was hybridized to Agilent's murine 4 × 44 k microarrays for 16 hours at 68°C and scanned using the Agilent DNA Microarray Scanner. Expression values were calculated by the software package Feature Extraction 10.5.1.1 (Agilent Technologies). Statistical analysis of the expression data was performed using the Gene Spring Software package (Agilent Technologies). Raw data were analyzed further using R package Limma. Raw data were $\log_2$-transformed and quantile-normalized.[36] All clustering was performed using the Bioconductor package ComplexHeatmap.[37] GSEA were conducted using the R version of the GSEA software provided by github of the Broad Institutes (https://github.com/GSEA-MSigDB/GSEA_R).[38]

Monoclonal Antibody Fas Injection and Caspase-3 Activity Assay

Ten-week-old mice on 100% NTBC or 14 days after NTBC withdrawal received an intraperitoneal injection with a monoclonal anti-Fas antibody (Jo2 purified anti-mouse CD95, 0.6 μg/g body weight diluted in 200 μL phosphate-buffered saline). Six hours after the injection, mice were killed and their livers were explanted. Caspase-3 activity was assayed using a synthetic tetrapeptide fluorogenic substrate (Ac-DEVD-AMC; BD Bioscience, San Jose, CA) in the presence or absence of the pan-caspase inhibitor (Ac-DEVD-CHO; BD Pharmingen), according to the manufacturer's recommendations.

One-Third Partial Hepatectomy

Mice were anesthetized with an intraperitoneal injection of Ketanest/Rompun (Bayer, Leverkusen, Germany). An abdominal midline incision was performed and the liver was exposed. After ligation, the left liver lobe was resected. The abdominal wall was sutured and mice recovered from anesthesia on a warming pad.

Histology and Immunostaining

Liver tissue was fixed in 3.5%–3.7% formaldehyde, processed, and paraffin-embedded. Sections (5 μm) were stained with H&E or processed further for immunohistochemistry. Ki67 (ab16667, 1:200; Abcam, Cambridge, UK), p21 (ab188224, 1:500; Abcam), and ß-catenin (ab6302, 1:100; Abcam) staining were performed using standard immunohistochemistry protocols. TUNEL staining was performed according to the manufacturer's protocols (Roche Diagnostics GmbH, Mannheim, Germany).

GSH/GSSG Measurements

Total glutathione (GSH + GSSG) and GSSG were measured as described.[1]

Immunoblotting

Frozen liver tissue was homogenized using an Ultra-Turrax (IKA, Staufen, Germany) for 10 seconds in AMP-activated protein kinase lysis buffer (50 mmol/L HEPES, 50 mmol/L KCl, 50 mmol/L Natrium fluorid, 5 mmol/L Sodium pyrophosphate decahydrate, 1 mmol/L EDTA, 1 mmol/L ethylene glycol-bis(β-aminoethyl ether)-*N,N,N′,N′*-tetra-acetic acid, 5 mmol/L ß-glycerophosphate, 1 mmol/L dithiothreitol, 1 mmol/L sodium orthovanadate, and 1% [v/v] Nonidet P40) containing Complete Protease Inhibitor mixture (Roche, Germany) and centrifuged for 10 minutes at 16,000 $\times$ g. All antibodies were used at 1:1000 dilutions unless otherwise indicated.

C-jun (9165), cleaved caspase-3 (9664), Flip (3210), p38 (9212), phospho-Jnk (Thr193/Tyr185) (9251), phospho-ribosomal protein S6 (Ser240/244) (5364, 1:500, bovine serum albumin), and vinculin (13901, 1:2000) were from Cell Signaling (Leiden, Netherland).

BCL2-associated X protein (sc-493), FAS (sc-716), and glyceraldehyde-3-phosphate dehydrogenase (sc-32233) were from Santa Cruz Biotechnology Inc. (Heidelberg, Germany). BCL2-like 1 (610211; BD Biosciences), Bcl-2 homology 3 interacting domain death agonist at 1:2000 (AF860; Bio-Techne GmbH, formerly R&D Systems, Wiesbaden-Nordenstadt, Germany), BCL2-like 11 (apoptosis facilitator) (B7929; Sigma-Aldrich Chemie GmbH, Taufkirchen, Germany), CASP8 and FADD-like apoptosis regulator (AAP-440; Stressgen), heme oxygenase 1 (ADI-SPA-896F, 1:500; Enzo Life Sciences GmbH, Lörrach, Germany), and myeloid cell leukemia sequence 1 (Mcl-1) (600-401-394; Rockland Immunochemicals Inc, Limerick, PA) also were used.

Cyclin D1 (ab134175, 1:500), glutamate cysteine ligase, catalytic subunit (ab53179, 1:500), glutamate cysteine ligase, modifier subunit (ab153967, 1:500), reduced nicotinamide adenine dinucleotide phosphate dehydrogenase, quinone 1 (ab80588, 1:500), p21 (ab188224, 1:500) phospho-RB S780 (ab184702), and phospho-RB S807 (ab184796) were from Abcam.

Horseradish-peroxidase–conjugated secondary antibodies were purchased from Santa Cruz Biotechnologies (sc-2357) and Cell Signaling (7074).

IP

For IP we used the Pierce Classic IP Kit (26146, Fisher Scientific GmbH, Part of Thermo Fisher Scientific, Schwerte, Germany) according to the manufacturer's protocol. Frozen liver tissue (50 mg) was homogenized using an Ultra-Turrax (IKA) for 10 seconds in the lysis buffer contained in the kit, to which we added Complete Protease Inhibitor mixture (Roche) and phosphatase inhibitors (2.5 mmol/L sodium pyrophosphate, 1 mmol/L ß-glycerophosphate, and 1 mmol/L sodium orthovanadate). For immune complex formation we used 5 μg of a purified antibody and 500 μg precleared liver lysate. The following antibodies from Abcam (UK) were used: CDK2 (ab32147), CDK4 (ab199728), cyclin D1 (ab134175) p21 (ab188224), and p27 (ab190851). For antibody detection, the Clean-Blot IP Detection Reagent from Thermo Scientific (21230) was used.

Transaminase Levels

Blood was collected in lithium heparin tubes (LH1.3; SARSTEDT AG & Co. KG (Nümbrecht, Germany), Olympus Deutschland GmbH (Hamburg, Germany) and transaminase activity was measured using an Olympus AU 400 System (Olympus, Germany).

RNA Isolation and Quantitative Polymerase Chain Reaction

Total RNA was extracted from liver tissue (n = 4) using the NucleoSpin RNA II kit (Macherey-Nagel GmbH & Co KG, Düren, Germany) and complementary DNA was synthesized using the Transcriptor High Fidelity Complementary DNA Kit (Roche). The relative quantification of gene expression was performed by TaqMan Gene Expression Assay in a QuantStudio 12K Flex Real-Time Polymerase Chain Reaction System (Fisher Scientific) according to the manufacturer's

protocol. Glyceraldehyde-3-phosphate dehydrogenase served as an internal control. The following TaqMan (Life Technologies GmbH Darmstadt, Germany) probes were used: Mm00432359_m1 (Ccnd1), Mm00432448_m1 (p21), and Mm99999915_g1 (glyceraldehyde-3-phosphate dehydrogenase).

aCGH

Agilent oligonucleotide aCGH for genomic DNA analysis (SurePrint G3 Mouse CGH Microarray Kit 4 × 180K; Agilent Technologies, Santa Clara, CA) was performed on frozen tumor tissue. Isolated genomic DNA (1 μg) was digested and labeled by random priming with cyanine 5-deoxyuridine triphosphate (tumor DNA) or cyanine 3-deoxyuridine triphosphate (reference DNA) using the SureTag DNA Labeling Kit (Agilent Technologies) according to the manufacturer's protocol. As reference, spleen genomic DNA was used. Microarray slides were scanned using a G2565CA microarray scanner (Agilent Technologies), and raw data were extracted using the Feature Extraction software (v.10.7.3.1; Agilent Technologies) for further analyses with the Genomic Workbench software (v.7.0.4.0; Agilent Technologies). The extracted files were analyzed with the statistical algorithm ADM-2.

Statistical Analysis

Data are represented as means ± SEM or as medians in box-and-whisker plots (Tukey test). Data were analyzed by analysis of variance, followed by the Student t test to determine significance. P values were considered statistically significant when $P \leq .05$.

References

1. Plentz RR, Park YN, Lechel A, Kim H, Nellessen F, Langkopf BH, Wilkens L, Destro A, Fiamengo B, Manns MP, Roncalli M, Rudolph KL. Telomere shortening and inactivation of cell cycle checkpoints characterize human hepatocarcinogenesis. Hepatology 2007; 45:968–976.
2. Katz SF, Lechel A, Obenauf AC, Begus-Nahrmann Y, Kraus JM, Hoffmann EM, Duda J, Eshraghi P, Hartmann D, Liss B, Schirmacher P, Kestler HA, Speicher MR, Rudolph KL. Disruption of Trp53 in livers of mice induces formation of carcinomas with bilineal differentiation. Gastroenterology 2012;142:1229–1239 e3.
3. Willenbring H, Sharma AD, Vogel A, Lee AY, Rothfuss A, Wang Z, Finegold M, Grompe M. Loss of p21 permits carcinogenesis from chronically damaged liver and kidney epithelial cells despite unchecked apoptosis. Cancer Cell 2008;14:59–67.
4. Boege Y, Malehmir M, Healy ME, Bettermann K, Lorentzen A, Vucur M, Ahuja AK, Bohm F, Mertens JC, Shimizu Y, Frick L, Remouchamps C, Mutreja K, Kahne T, Sundaravinayagam D, Wolf MJ, Rehrauer H, Koppe C, Speicher T, Padrissa-Altes S, Maire R, Schattenberg JM, Jeong JS, Liu L, Zwirner S, Boger R, Huser N, Davis RJ, Mullhaupt B, Moch H, Schulze-Bergkamen H, Clavien PA, Werner S, Borsig L, Luther SA, Jost PJ, Weinlich R, Unger K, Behrens A, Hillert L, Dillon C, Di Virgilio M, Wallach D, Dejardin E, Zender L, Naumann M, Walczak H, Green DR, Lopes M, Lavrik I, Luedde T, Heikenwalder M, Weber A. A dual role of caspase-8 in triggering and sensing proliferation-associated DNA damage, a key determinant of liver cancer development. Cancer Cell 2017;32:342–359 e10.
5. Kastenhuber ER, Lowe SW. Putting p53 in context. Cell 2017;170:1062–1078.
6. Teoh N, Pyakurel P, Dan YY, Swisshelm K, Hou J, Mitchell C, Fausto N, Gu Y, Farrell G. Induction of p53 renders ATM-deficient mice refractory to hepatocarcinogenesis. Gastroenterology 2010;138:1155–1165, e1–2.
7. Hirao A, Kong YY, Matsuoka S, Wakeham A, Ruland J, Yoshida H, Liu D, Elledge SJ, Mak TW. DNA damage-induced activation of p53 by the checkpoint kinase Chk2. Science 2000;287:1824–1827.
8. Hirao A, Cheung A, Duncan G, Girard PM, Elia AJ, Wakeham A, Okada H, Sarkissian T, Wong JA, Sakai T, De Stanchina E, Bristow RG, Suda T, Lowe SW, Jeggo PA, Elledge SJ, Mak TW. Chk2 is a tumor suppressor that regulates apoptosis in both an ataxia telangiectasia mutated (ATM)-dependent and an ATM-independent manner. Mol Cell Biol 2002;22:6521–6532.
9. Zender L, Spector MS, Xue W, Flemming P, Cordon-Cardo C, Silke J, Fan ST, Luk JM, Wigler M, Hannon GJ, Mu D, Lucito R, Powers S, Lowe SW. Identification and validation of oncogenes in liver cancer using an integrative oncogenomic approach. Cell 2006; 125:1253–1267.
10. McClendon AK, Dean JL, Ertel A, Fu Z, Rivadeneira DB, Reed CA, Bourgo RJ, Witkiewicz A, Addya S, Mayhew CN, Grimes HL, Fortina P, Knudsen ES. RB and p53 cooperate to prevent liver tumorigenesis in response to tissue damage. Gastroenterology 2011; 141:1439–1450.
11. Borude P, Bhushan B, Gunewardena S, Akakpo J, Jaeschke H, Apte U. Pleiotropic role of p53 in injury and liver regeneration after acetaminophen overdose. Am J Pathol 2018;188:1406–1418.
12. Sun J, Wen Y, Zhou Y, Jiang Y, Chen Y, Zhang H, Guan L, Yao X, Huang M, Bi H. p53 attenuates acetaminophen-induced hepatotoxicity by regulating drug-metabolizing enzymes and transporter expression. Cell Death Dis 2018;9:536.
13. Tomita K, Teratani T, Suzuki T, Oshikawa T, Yokoyama H, Shimamura K, Nishiyama K, Mataki N, Irie R, Minamino T, Okada Y, Kurihara C, Ebinuma H, Saito H, Shimizu I, Yoshida Y, Hokari R, Sugiyama K, Hatsuse K, Yamamoto J, Kanai T, Miura S, Hibi T. p53/p66Shc-mediated signaling contributes to the progression of non-alcoholic steatohepatitis in humans and mice. J Hepatol 2012;57:837–843.
14. Derdak Z, Villegas KA, Harb R, Wu AM, Sousa A, Wands JR. Inhibition of p53 attenuates steatosis and liver injury in a mouse model of non-alcoholic fatty liver disease. J Hepatol 2013;58:785–791.
15. Choudhury AR, Ju Z, Djojosubroto MW, Schienke A, Lechel A, Schaetzlein S, Jiang H, Stepczynska A, Wang C, Buer J, Lee HW, von Zglinicki T, Ganser A,

Schirmacher P, Nakauchi H, Rudolph KL. Cdkn1a deletion improves stem cell function and lifespan of mice with dysfunctional telomeres without accelerating cancer formation. Nat Genet 2007;39:99–105.
16. De la Cueva E, Garcia-Cao I, Herranz M, Lopez P, Garcia-Palencia P, Flores JM, Serrano M, Fernandez-Piqueras J, Martin-Caballero J. Tumorigenic activity of p21Waf1/Cip1 in thymic lymphoma. Oncogene 2006; 25:4128–4132.
17. Buitrago-Molina LE, Marhenke S, Longerich T, Sharma AD, Boukouris AE, Geffers R, Guigas B, Manns MP, Vogel A. The degree of liver injury determines the role of p21 in liver regeneration and hepatocarcinogenesis in mice. Hepatology 2013;58:1143–1152.
18. Grompe M, Lindstedt S, al-Dhalimy M, Kennaway NG, Papaconstantinou J, Torres-Ramos CA, Ou CN, Finegold M. Pharmacological correction of neonatal lethal hepatic dysfunction in a murine model of hereditary tyrosinaemia type I. Nat Genet 1995; 10:453–460.
19. Buitrago-Molina LE, Pothiraju D, Lamle J, Marhenke S, Kossatz U, Breuhahn K, Manns MP, Malek N, Vogel A. Rapamycin delays tumor development in murine livers by inhibiting proliferation of hepatocytes with DNA damage. Hepatology 2009;50:500–509.
20. Marhenke S, Lamle J, Buitrago-Molina LE, Canon JM, Geffers R, Finegold M, Sporn M, Yamamoto M, Manns MP, Grompe M, Vogel A. Activation of nuclear factor E2-related factor 2 in hereditary tyrosinemia type 1 and its role in survival and tumor development. Hepatology 2008;48:487–496.
21. Endig J, Buitrago-Molina LE, Marhenke S, Reisinger F, Saborowski A, Schutt J, Limbourg F, Konecke C, Schreder A, Michael A, Misslitz AC, Healy ME, Geffers R, Clavel T, Haller D, Unger K, Finegold M, Weber A, Manns MP, Longerich T, Heikenwalder M, Vogel A. Dual role of the adaptive immune system in liver injury and hepatocellular carcinoma development. Cancer Cell 2016;30:308–323.
22. Vogel A, van Den Berg IE, Al-Dhalimy M, Groopman J, Ou CN, Ryabinina O, Iordanov MS, Finegold M, Grompe M. Chronic liver disease in murine hereditary tyrosinemia type 1 induces resistance to cell death. Hepatology 2004;39:433–443.
23. Vogel A, Aslan JE, Willenbring H, Klein C, Finegold M, Mount H, Thomas G, Grompe M. Sustained phosphorylation of Bid is a marker for resistance to Fas-induced apoptosis during chronic liver diseases. Gastroenterology 2006;130:104–119.
24. Sherr CJ, Roberts JM. CDK inhibitors: positive and negative regulators of G1-phase progression. Genes Dev 1999;13:1501–1512.
25. Schungel S, Buitrago-Molina LE, Nalapareddy P, Lebofsky M, Manns MP, Jaeschke H, Gross A, Vogel A. The strength of the Fas ligand signal determines whether hepatocytes act as type 1 or type 2 cells in murine livers. Hepatology 2009;50:1558–1566.
26. Marhenke S, Buitrago-Molina LE, Endig J, Orlik J, Schweitzer N, Klett S, Longerich T, Geffers R, Sanchez Munoz A, Dorrell C, Katz SF, Lechel A, Weng H, Krech T, Lehmann U, Dooley S, Rudolph KL, Manns MP, Vogel A. p21 promotes sustained liver regeneration and hepatocarcinogenesis in chronic cholestatic liver injury. Gut 2014;63:1501–1512.
27. Liberzon A, Birger C, Thorvaldsdottir H, Ghandi M, Mesirov JP, Tamayo P. The Molecular Signatures Database (MSigDB) hallmark gene set collection. Cell Syst 2015;1:417–425.
28. Jorquera R, Tanguay RM. Fumarylacetoacetate, the metabolite accumulating in hereditary tyrosinemia, activates the ERK pathway and induces mitotic abnormalities and genomic instability. Hum Mol Genet 2001; 10:1741–1752.
29. Jorquera R, Tanguay RM. The mutagenicity of the tyrosine metabolite, fumarylacetoacetate, is enhanced by glutathione depletion. Biochem Biophys Res Commun 1997;232:42–48.
30. Gordon EM, Ravicz JR, Liu S, Chawla SP, Hall FL. Cell cycle checkpoint control: the cyclin G1/Mdm2/p53 axis emerges as a strategic target for broad-spectrum cancer gene therapy - a review of molecular mechanisms for oncologists. Mol Clin Oncol 2018;9:115–134.
31. Jensen MR, Factor VM, Thorgeirsson SS. Regulation of cyclin G1 during murine hepatic regeneration following Dipin-induced DNA damage. Hepatology 1998; 28:537–546.
32. Zhao L, Samuels T, Winckler S, Korgaonkar C, Tompkins V, Horne MC, Quelle DE. Cyclin G1 has growth inhibitory activity linked to the ARF-Mdm2-p53 and pRb tumor suppressor pathways. Mol Cancer Res 2003; 1:195–206.
33. Chen JJ, Yang T, Song SH, Liu QG, Sun Y, Zhao LH, Fu ZR, Wang MJ, Hu YP, Chen F. Senescence suppressed proliferation of host hepatocytes is precondition for liver repopulation. Biochem Biophys Res Commun 2019;516:591–598.
34. Wang C, Chen WJ, Wu YF, You P, Zheng SY, Liu CC, Xiang D, Wang MJ, Cai YC, Zhao QH, Borjigin U, Liu W, Xiong WJ, Wangensteen KJ, Wang X, Liu ZM, He ZY. The extent of liver injury determines hepatocyte fate toward senescence or cancer. Cell Death Dis 2018; 9:575.
35. Grompe M, Al-Dhalimy M, Finegold M, Ou CN, Burlingame T, Kennaway NG, Soriano P. Loss of fumarylacetoacetate hydrolase is responsible for the neonatal hepatic dysfunction phenotype of lethal albino mice. Genes Dev 1993;7:2298–2307.
36. Smyth GK. Linear models and empirical bayes methods for assessing differential expression in microarray experiments. Stat Appl Genet Mol Biol 2004;3, article 3.
37. Gu Z, Eils R, Schlesner M. Complex heatmaps reveal patterns and correlations in multidimensional genomic data. Bioinformatics 2016;32:2847–2849.
38. Subramanian A, Tamayo P, Mootha VK, Mukherjee S, Ebert BL, Gillette MA, Paulovich A, Pomeroy SL, Golub TR, Lander ES, Mesirov JP. Gene set enrichment analysis: a knowledge-based approach for interpreting genome-wide expression profiles. Proc Natl Acad Sci U S A 2005;102, 15545–1550.

Received September 8, 2020. Accepted January 12, 2021.

Correspondence
Address correspondence to: Arndt Vogel, MD, Department of Gastroenterology, Hepatology, and Endocrinology, Hannover Medical School, Carl-Neuberg-Str. 1, 30625 Hannover, Germany. e-mail: vogel.arndt@mh-hannover.de; fax: (49) 5115328392.

Acknowledgments
The authors thank Eric Jende and Meriame Nassiri for their expert technical assistance.

CRediT Authorship Contributions
Laura Elisa Buitago-Molina, PhD (Conceptualization: Equal; Formal analysis: Equal; Investigation: Equal; Writing – review & editing: Equal)
Silke Marhenke, PhD (Conceptualization: Equal; Formal analysis: Equal; Investigation: Equal; Writing – review & editing: Equal)
Diana Becker (Formal analysis: Equal; Investigation: Equal)
Robert Geffers, PhD (Formal analysis: Equal; Investigation: Equal)
Timo Itzel (Formal analysis: Equal)
Andreas Teufel, MD/ PhD (Formal analysis: Equal)
Hartmut Jaeschke, PhD (Formal analysis: Equal; Investigation: Supporting)
André Lechel, PhD (Formal analysis: Equal; Investigation: Supporting; Resources: Supporting; Writing – review & editing: Supporting)
Kristian Unger, PhD (Formal analysis: Equal)
Jens U. Marquardt, MD (Formal analysis: Supporting; Writing – review & editing: Supporting)
Michael Saborowski, MD (Conceptualization: Supporting; Formal analysis: Supporting; Writing – review & editing: Supporting)
Anna Saborowski, MD (Conceptualization: Equal; Formal analysis: Equal; Funding acquisition: Supporting; Project administration: Equal; Writing – original draft: Lead)
Arndt Vogel, MD (Conceptualization: Lead; Formal analysis: Equal; Funding acquisition: Lead; Project administration: Lead; Supervision: Lead; Writing – original draft: Lead)

Conflicts of interest
The authors disclose no conflicts.

Funding
This work was funded by the Deutsche Forschungsgemeinschaft (German Research Foundation) grants SFB/TR 209–314905040 (A.S., A.V., M.S.), grant BU2722/2-3 (L.E.B-M) and Vo959/9-1 (A.V.) and supported by Else Kröner-Fresenius Foundation grant 2015_A225 (A.S.).